Calibration of Lévy Option Pricing Models: Application to S&P 500 Futures Option

Kazuhisa Matsuda

Department of Economics
The Graduate Center, The City University of New York,
365 Fifth Avenue, New York, NY 10016-4309
Phone: (718) 288-6704
Email: maxmatsuda@hotmail.com
http://www.maxmatsuda.com/

First Draft: June 24 2005
This version: August 23, 2005

Calibration of Lévy Option Pricing Models: Application to S&P 500 Futures Option

Abstract

The trend since the mid 90's in option pricing is the elimination of a Browian motion in the underlying asset price stochastic process. This implies the transition from continuous sample paths to pure jump sample paths. This paper calibrates the five different Lévy models to the S&P 500 futures options and compares their pricing performance and the implied dynamics. The result shows that jump Lévy models drastically outperform the classic Black-Scholes model in pricing. Introduction of extra parameters of jump Lévy models turned out to allow the negative skewness and the excess kurtosis of the log return density.

1. Introduction

Since the mid 1990's, there was an explosion of literatures regarding so called pure jump Lévy models which try to model the stochastic process of the underlying asset price with pure jump Lévy processes. Matsuda (2005a) defines a Lévy process as follows.

Definition 1 Lévy processes A real valued stochastic process $(X_{t\in[0,\infty)})$ on a filtered probability space $(\Omega, \mathcal{F}_{t\in[0,\infty)}, \mathbb{P})$ is said to be a Lévy process on $\mathbb{R}$ if it satisfies the following conditions:

(1) Its increments are independent. In other words, for $0 \le t_1 < t_2 < ... < t_n < \infty$:

$$\mathbb{P}(X_{t_0} \bigcap X_{t_1} - X_{t_0} \bigcap X_{t_2} - X_{t_1} \bigcap ... \bigcap X_{t_n} - X_{t_{n-1}})$$

$$= \mathbb{P}(X_{t_0})\mathbb{P}(X_{t_1} - X_{t_0})\mathbb{P}(X_{t_2} - X_{t_1})...\mathbb{P}(X_{t_n} - X_{t_{n-1}}).$$

(2) Its increments are stationary (time homogeneous): i.e. for $h \ge 0$, $X_{t+h} - X_t$ has the same distribution as X_h. In other words, the distribution of increments does not depend on t.

(3) $\mathbb{P}(X_0 = 0) = 1$. The process starts from 0 almost surely (with probability 1).

(4) The process is stochastically continuous: $\forall \varepsilon > 0$, $\lim_{h\to 0} \mathbb{P}(|X_{t+h} - X_t| \ge \varepsilon) = 0$.

(5) Its sample path (trajectory) is right continuous with left limit (i.e. rcll) almost surely.

Processes satisfying the conditions (1) and (2) are called processes with independent and stationary increments. Independent increments condition is a restriction on the probabilistic dependence structure of increments among the past, present, and future. Stationary increments condition is a restriction on the shape of the distribution of increments among the past, present, and future. The condition (4) (which is implied by the conditions (2), (3), and (5)) does not imply the continuous sample paths of the

process. It means that if we are at time t, the probability of a jump at time t is zero because there is no uncertainty about the present. Jumps occur at random times. This property is called stochastic continuity or continuity in probability. Rcll condition (5) does not need to be imposed. This is because a real valued Lévy process in law which is a process satisfying conditions (1), (2), (3), and (4) is modified to a Lévy process which satisfies the conditions (1), (2), (3), (4) , and (5) (theorem 11.5 of Sato (1999)). In other words, the condition (5) results from the conditions (1), (2), (3), and (4) through a theorem. As you can see, the fact that left continuity is not needed allows the process to have jumps. A continuous stochastic process implies a rcll stochastic process but the reverse is not true. All stochastic processes used in finance literatures for the modeling of asset price dynamics are rcll stochastic processes. Rcll processes include jump discontinuous process such as Poisson processes and infinite activity Lévy processes.

Let $(L_{t\in[0,T]})$ be a Lévy process defined on a filtered risk-neutral probability space $(\Omega, \mathcal{F}_{t\in[0,T]}, \mathbb{Q})$. Lévy models specify the dynamics of an increment of an underlying asset price as:

$$dS = rSdt + SdL.$$

This means that the classic BS model is a Lévy model when the choice of a Lévy process is a multiplicative Brownian motion:

$$(L_{t\in[0,T]}) \equiv (\sigma B_{t\in[0,T]}).$$

It turns out that a Brownian motion is the only Lévy process with continuous sample paths. This continuous sample paths property of the underlying price is another defect of the BS model which is not supported by the empirical evidence. It is a well established fact that asset prices do jump especially in the downward direction. The first jump Lévy

model was developed by Merton (1976). Merton simply adds a compound Poisson process which is a pure jump Lévy process to the Brownian motion. Addition of a compound Poisson process allows the asset price to have rare jumps.

In contrast to the MJD (Merton jump diffusion) model which possesses mostly continuous with rare discontinuous sample paths, more recent Lévy models possess pure jump sample paths. They are labeled as pure jump Lévy models or purely non-Gaussian Lévy models. Carr, Chang, and Madan (1998) developed the variance gamma (VG) model, Barndorff-Nielsen created the normal inverse Gaussian (NIG) model, and Carr, Geman, Madan, and Yor (2002) developed the CGMY model. Pure jump Lévy models are probably the most drastic revolution in the finance literature since the BS model because they no longer contain a Brownian motion. Note that the well-studied and popular stochastic volatility models which introduce extra parameters by making the volatility random and these extra parameters control the non-normality of log returns still contain a Brownian motion. Consult Hull and White (1987) and Heston (1993) for stochastic volatility models. In contrast to modeling the volatility, the pure jump Lévy models specify the underlying asset price process as pure jump Lévy processes introducing parameters which control the non-normality of log returns.

The goal of this paper is to give an answer to the following simple question, “What do we gain by allowing the asset price process to jump or by specifying the asset price process as a pure jump Lévy process?” For this purpose, we calibrate a total of five different Lévy models to the S&P 500 futures options. The gain of jump Lévy models over the BS model is judged by two main criterions. One is the implied dynamics of the log return probability density and the Lévy density. The other is the out-of-sample fit of

the each Lévy model following Bakshi, Cao, and Chen (1997) because of the fact that the better in-sample fit might be due to more parameters of the jump Lévy models than the BS model. In other words, if the extra parameters of the jump Lévy models are redundant, they overfit the data and may produce larger out-of-sample fitting errors.

The calibration result based on 6567 call option prices on S&P 500 futures with March 2005 maturity for the sample period from March 24, 2004, through March 16, 2005 suggests that the extra parameters of various jump Lévy models allow the negative skewness and the excess kurtosis of the log return density over the BS model. On the dynamics of implied Lévy density functions of log returns, the pattern of increasing total mass of the MJD model's symmetric Lévy density is observed. Lévy densities of all pure jump Lévy models are characterized by the asymmetric and infinite activity Lévy densities which all resemble one another. Containing jumps in the underlying price process drastically improves the out-of-sample pricing performance over the BS model. As expected, the BS model is characterized by the bias of underpricing the ITM calls and overpricing the OTM calls. Among jump Lévy models, the CGMY model turned out to be the best performing model for the overall option pricing although it is outperformed by the NIG, MJD, and VG models for the short term deep out-of-the money calls.

This paper is organized as follows. Section 2 presents three pure jump (i.e. purely non-Gaussian) Lévy models in which the asset price dynamics is modeled using pure jump Lévy process. Section 3 reviews the Gaussian Lévy model and the non-Gaussian Lévy model. Section 4 describes the S&P 500 futures option data set and our calibration methodology. Section 5 provides the implied dynamics of the probability density and the Lévy measure of the log returns. In-sample pricing performance of each model is

discussed. Section 6 evaluates the out-of-sample pricing performance of each model. Section 7 concludes.

2. Pure Jump Lévy Models

In this section, we present three pure jump Lévy models in which the asset price dynamics is modeled using pure jump Lévy process. Intuitively, this means that the asset price moves only by jumps (i.e. discontinuities). Pure jump Lévy processes are also called as purely non-Gaussian Lévy processes because they have zero Gaussian variance following Lévy-Itô decomposition of the sample paths. There are several different ways of building pure jump Lévy processes[a]. The variance gamma process and the normal inverse Gaussian process which are described in section 2.1 and 2.2 are the class of Lévy process called the subordinated Brownian motion with the tempered stable subordinator. The CGMY model in section 2.3 builds the Lévy process by specifying the Lévy measure and the use of Lévy-Khinchin representation.

2.A Variance Gamma Model by Carr, Chang, and Madan (1998)

Consider a fixed filtered probability space $(\Omega, \mathcal{F}_{t\in[0,\infty)}, \mathbb{P})$. Let $(W_{t\in[0,\infty)}) \equiv (\theta t + \sigma B_{t\in[0,\infty)})$ be a Brownian motion with drift where $(B_{t\in[0,\infty)})$ is a standard Brownian motion. Let $(Z_{t\in[0,\infty)})$ be the gamma subordinator[b] with unit mean rate[c] with the Lévy triplet $(A_Z = 0, \ell_Z, \gamma_Z = 0)$ whose probability density is one parameter family of the variance rate $\nu \in \mathbb{R}^+$:

$$\mathbb{P}_G(z_t;\nu) = \frac{z^{\frac{t}{\nu}-1}\exp\left(-\frac{z}{\nu}\right)}{\nu^{\frac{t}{\nu}}\Gamma\left(\frac{t}{\nu}\right)}1_{z>0}, \tag{1}$$

[a] We recommend Cont and Tankov (2004).

[b] Subordinator is defined as an increasing Lévy process.

[c] Consult Appendix 1.

its characteristic function[d] is:

$$\phi_Z(\omega) = \frac{1}{\left(1 - i\omega\nu\right)^{\frac{t}{\nu}}}, \tag{2}$$

and its moment generating function[e] is:

$$M_Z(\omega) = \frac{1}{\left(1 - \omega\nu\right)^{\frac{t}{\nu}}} = \exp\left(t\mathcal{L}_Z(\omega)\right), \tag{3}$$

where the Laplace exponent is given by:

$$\mathcal{L}_Z(\omega) = -\frac{1}{\nu}\ln\left(1 - \omega\nu\right). \tag{4}$$

Assume the statistical independence between $(W_{t\in[0,\infty)})$ and $(Z_{t\in[0,\infty)})$. Then, the variance gamma (VG) process $(X_{t\in[0,\infty)})$ is defined as a subordinated Brownian motion with the gamma subordinator with unit mean rate:

$$X(t,\omega) \equiv W(Z_t(\omega),\omega) \equiv \theta Z_t(\omega) + \sigma B(Z_t(\omega),\omega). \tag{5}$$

This VG process $(X_{t\in[0,\infty)})$ with the Lévy triplet $(A_X = 0, \ell_X, \gamma_X)$ defined on a filtered probability space $(\Omega, \mathcal{F}_{t\in[0,\infty]}, \mathbb{P})$ possesses the following properties. It is a pure jump Lévy process (i.e. a purely non-Gaussian Lévy process) which is equivalent to stating that the Gaussian variance term is zero $A_X = 0$ following the Lévy-Itô decomposition of the

[d] Characteristic function is defined as the Fourier transform of the probability density function $\mathbb{P}(x)$, i.e. $\phi_X(\omega) \equiv \int_{-\infty}^{\infty} \mathrm{e}^{i\omega x}\mathbb{P}(x)dx$.

[e] Moment generating function is defined as $M_X(\omega) \equiv \int_{-\infty}^{\infty} \mathrm{e}^{\omega x}\mathbb{P}(x)dx$.

sample paths. Its characteristic function can be obtained by the use of the subordination theorem of Lévy processes which corresponds to Theorem 30.1 of Sato (1999):

$$\phi_X(\omega) \equiv \int_{-\infty}^{\infty} \mathrm{e}^{i\omega x} \mathbb{P}(x) dx = \exp\left\{ t \mathcal{L}_Z\left(\psi_W(\omega)\right)\right\}, \tag{6}$$

where $\psi_W(\omega)$ is the characteristic exponent of the Brownian motion with drift:

$$\psi_W(\omega) = i\theta\omega - \frac{\sigma^2\omega^2}{2}. \tag{7}$$

Substitution of (4) and (7) into (6) produces:

$$\phi_{VG,X}(\omega;\theta,\sigma,\nu) = \left(1 - i\nu\theta\omega + \frac{\nu\sigma^2\omega^2}{2}\right)^{-\frac{t}{\nu}}. \tag{8}$$

Its probability density is given by:

$$\mathbb{P}_{VG}(x_t;\theta,\sigma,\nu) = \frac{\sqrt{2}\exp\left(\frac{\theta}{\sigma^2}x_t\right)}{\nu^{t/\nu}\sigma\sqrt{\pi}\Gamma(t/\nu)}\left(\frac{x_t^{\,2}}{\frac{2\sigma^2}{\nu}+\theta^2}\right)^{\frac{t}{2\nu}-\frac{1}{4}} K_{\frac{t}{\nu}-\frac{1}{2}}\left(\frac{\sqrt{x_t^{\,2}\left(\frac{2\sigma^2}{\nu}+\theta^2\right)}}{\sigma^2}\right), \tag{9}$$

where K is the modified Bessel function of the second kind. Note that this probability density can be easily computed using the conditionally normal property of the VG process:

$$\mathbb{P}_{VG}(x_t;\theta,\sigma,\nu) = \int_0^{\infty} VG(x_t \,|\, t = z_t = z)\mathbb{P}_G(z_t;\nu)dz$$

$$\mathbb{P}_{VG}(x_t;\theta,\sigma,\nu) = \int_0^{\infty} \frac{1}{\sqrt{2\pi\sigma^2 z}}\exp\left\{-\frac{(x_t-\theta z)^2}{2\sigma^2 z}\right\}\frac{z^{\frac{t}{\nu}-1}\exp\left(-\frac{z}{\nu}\right)}{\nu^{\frac{t}{\nu}}\Gamma\left(\frac{t}{\nu}\right)}dz.$$

Its standardized moments are computed by:

$$E[X_t] = \theta t, \tag{10}$$

$$Variance[X_t] = (\nu\theta^2 + \sigma^2)t\,,$$

$$Skewness[X_t] = \frac{\nu\theta(2\nu\theta^2 + 3\sigma^2)}{\sqrt{t}(\nu\theta^2 + \sigma^2)^{3/2}}\,,$$

$$Excess\ Kurtosis[X_t] = \frac{3\nu(2\nu^2\theta^4 + 4\nu\theta^2\sigma^2 + \sigma^4)}{t(\nu\theta^2 + \sigma^2)^2}\,.$$

These standardized moments indicate that $\theta \in \mathbb{R}$ is a location and a skewness parameter, $\sigma \in \mathbb{R}^+$ is a shape parameter, and $\nu \in \mathbb{R}^+$ controls the tail behavior[f] of the probability density (and also the Lévy density) of the VG process.

The Lévy measure of the VG process is of the form:

(11) $$\ell_{VG,X}(x;\theta,\sigma,\nu) = \frac{1}{\nu|x|}\exp\left(\frac{\theta}{\sigma^2}x - \frac{|x|}{\sigma^2}\sqrt{\frac{2\sigma^2}{\nu} + \theta^2}\right).$$

The total mass of the Lévy measure of the VG process is infinite:

$$\int_{-\infty}^{\infty} \ell_{VG,X}(x)dx = \infty\,.$$

In other words, the VG process is an infinite activity Lévy process which means that the VG process has infinitely many small jumps and a finite number of large jumps inheriting the infinite arrival rate of jumps from the gamma subordinator. The VG process is also a Lévy process of finite variation in the interval $[0,\infty)$. In other words, it is a Lévy process satisfying:

$$A_X = 0 \text{ and } \int_{|x|<1} |x|\ell_{VG,X}(x)dx < \infty\,.$$

[f] The larger value of variance rate ν of the gamma subordinator $(Z_{t\in[0,\infty)})$ with unit mean rate (i.e. which determines the degree of randomness of the subordination) makes the probability density of the VG process fatter tailed and higher peaked (i.e. more leptokurtic).

Consult theorem 3.11 of Matsuda (2005a). Examples of the Lévy measure of the VG process (11) are plotted in Figure 1. The sign of $\theta \in \mathbb{R}$ determines the skewness of the VG Lévy measure as illustrated by Panel A. $\sigma \in \mathbb{R}^+$ controls its shape as shown by Panel B. Larger values of the variance rate $\nu \in \mathbb{R}^+$ of the gamma subordinator[g] make the tails of the Lévy measure fatter which indicates the higher arrival rate of large jumps as depicted by Panel C.

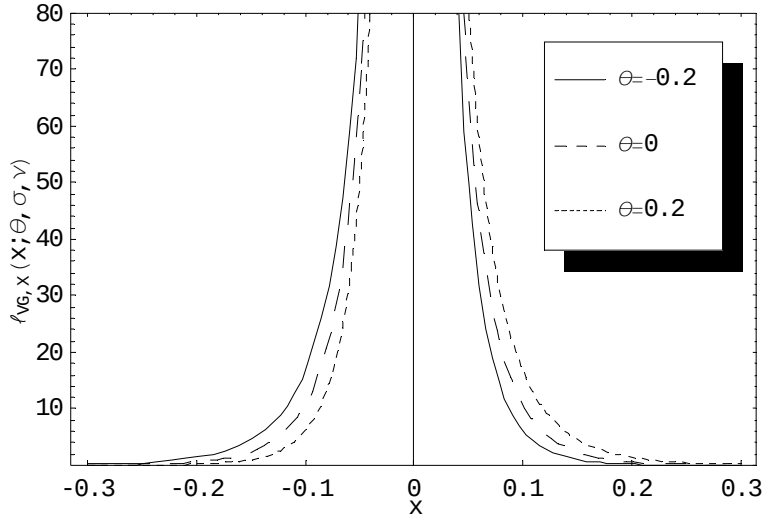

A) Lévy measure of VG process with various values for θ Parameters fixed are $\sigma = 0.2$ and $\nu = 0.1$.

[g] Which indicates the higher degree of randomness of the subordination.

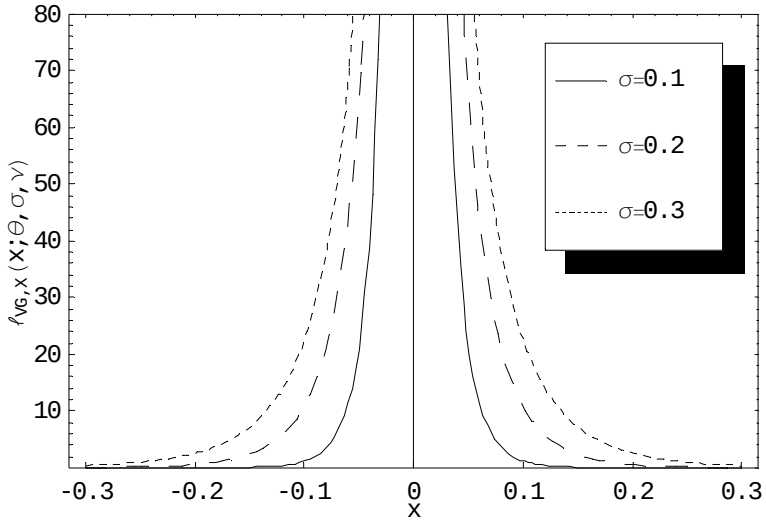

B) Lévy measure of VG process with various values for σ Parameters fixed are $\theta = 0$ and $\nu = 0.1$.

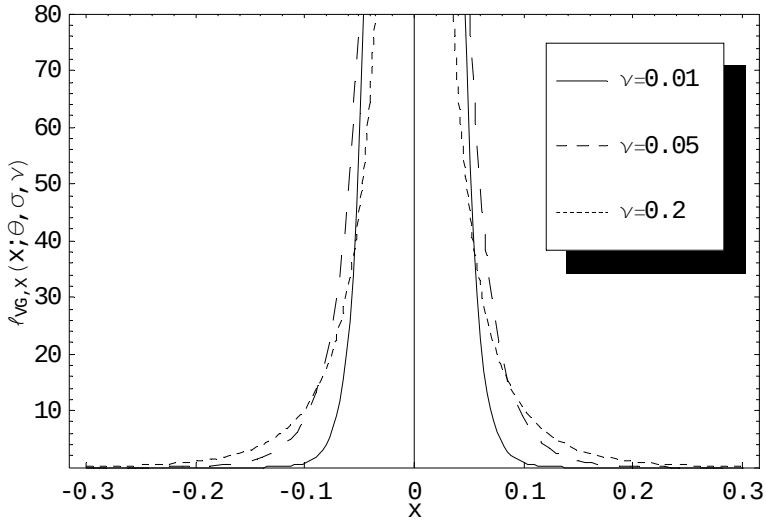

C) Lévy measure of VG process with various values for ν Parameters fixed are $\theta = 0$ and $\sigma = 0.2$.

Figure 1 Plot of Lévy measure $\ell_{VG,X}(x;\theta,\sigma,\nu)$ of VG process

The VG model specifies the asset price dynamics $(S_{t\in[0,T]})$ defined on a filtered risk neutral probability space $(\Omega, \mathcal{F}_{t\in[0,T]}, \mathbb{Q})$ as an exponential (geometric) of a Lévy process $(L_{t\in[0,T]})$:

$$S_t = S_0 \exp(L_t),$$

where the choice of the Lévy process is the VG process plus the drift $r - \varpi_{VG,\mathbb{Q}}$:

$$L_t \equiv (r - \varpi_{VG,\mathbb{Q}})t + VG(x_t; \theta_{\mathbb{Q}}, \sigma_{\mathbb{Q}}, \nu_{\mathbb{Q}}), \tag{12}$$

where $r \in \mathbb{R}^+$ is the instantaneous risk-free interest rate and all parameters are under the risk neutral probability measure $\mathbb{Q}$. The term $\varpi_{VG,\mathbb{Q}}$ is the convexity correction[h] which takes the following form in the VG model:

$$\varpi_{VG,\mathbb{Q}} \equiv -\frac{1}{\nu_{\mathbb{Q}}} \ln\left(1 - \theta_{\mathbb{Q}}\nu_{\mathbb{Q}} - \frac{{\sigma_{\mathbb{Q}}}^2 \nu_{\mathbb{Q}}}{2}\right). \tag{13}$$

Define the log return (i.e. log price relative) of the asset price as:

$$R_t \equiv \ln(S_t / S_0). \tag{14}$$

Then, from the equation (12):

$$x_t = R_t - (r - \varpi_{VG,\mathbb{Q}})t. \tag{15}$$

Since obviously the drift $r - \varpi_{VG,\mathbb{Q}}$ is deterministic, the probability density of the log return in the VG model under the risk neutral probability measure $\mathbb{Q}$ can be expressed using the density (9) as:

$$\mathbb{Q}_{VG}(R_t; \theta, \sigma, \nu) = \frac{\sqrt{2}\exp\left(\frac{\theta}{\sigma^2}x_t\right)}{\nu^{t/\nu}\sigma\sqrt{\pi}\Gamma(t/\nu)}\left(\frac{{x_t}^2}{\frac{2\sigma^2}{\nu} + \theta^2}\right)^{\frac{t}{2\nu}-\frac{1}{4}} K_{\frac{t}{\nu}-\frac{1}{2}}\left(\frac{\sqrt{{x_t}^2\left(\frac{2\sigma^2}{\nu} + \theta^2\right)}}{\sigma^2}\right), \tag{16}$$

---

[h] The convexity correction term ensures that the discounted asset price process $(e^{-rt}S_{t\in[0,T]})$ becomes a martingale under $\mathbb{Q}$, i.e. $E^{\mathbb{Q}}[e^{-rt}S_t \,|\, \mathcal{F}_t] = S_0$. To ensure this martingale condition, we must have $\exp(\varpi_{\mathbb{Q}}) = E^{\mathbb{Q}}\left\{\exp\left(VG(x_1; \theta_{\mathbb{Q}}, \sigma_{\mathbb{Q}}, \nu_{\mathbb{Q}})\right) \middle| \mathcal{F}_1\right\}$.

with the equation (15). Note that all parameters in the density (16) are under the risk neutral probability measure $\mathbb{Q}$.

2.B Normal Inverse Gaussian Model by Barndorff-Nielsen (1998)

Consider a fixed filtered probability space $(\Omega, \mathcal{F}_{t\in[0,\infty)}, \mathbb{P})$. Let $(W_{t\in[0,\infty)}) \equiv (\beta t + B_{t\in[0,\infty)})$ be a Brownian motion with drift where $(B_{t\in[0,\infty)})$ is a standard Brownian motion. Let $(Z_{t\in[0,\infty)})$ be the inverse Gaussian subordinator[i] with the Lévy triplet $(A_Z = 0, \ell_Z, \gamma_Z = 0)$ whose probability density is a two parameter family of $\delta \in \mathbb{R}^+$ and $\gamma \equiv \sqrt{\alpha^2 - \beta^2} \in \mathbb{R}^+$:

$$\mathbb{P}_{IG}(z_t;\delta,\gamma) = \frac{\delta t}{\sqrt{2\pi}} z_t^{-3/2} \exp(\delta\gamma t) \exp\left\{-\frac{\left(\gamma^2 z_t + \delta^2 t^2 z_t^{-1}\right)}{2}\right\} 1_{z>0}, \tag{17}$$

its characteristic function is:

$$\phi_Z(\omega) = \exp\left(\delta t\gamma - \delta t\sqrt{\gamma^2 - 2i\omega}\right), \tag{18}$$

and its moment generating function is:

$$M_Z(\omega) = \exp\left(\delta t\gamma - \delta t\sqrt{\gamma^2 - 2\omega}\right) = \exp\left(t\mathcal{L}_Z(\omega)\right), \tag{19}$$

where the Laplace exponent is given by:

$$\mathcal{L}_Z(\omega) = \delta\gamma - \delta\sqrt{\gamma^2 - 2\omega}. \tag{20}$$

Assume the statistical independence between $(W_{t\in[0,\infty)})$ and $(Z_{t\in[0,\infty)})$. Then, the normal inverse Gaussian (NIG) process $(X_{t\in[0,\infty)})$ is defined as a subordinated Brownian motion with the IG subordinator plus the drift $\mu \in \mathbb{R}$:

$$X(t,\omega) \equiv \mu t + W(Z_t(\omega),\omega) \equiv \mu t + \beta Z_t(\omega) + B(Z_t(\omega),\omega). \tag{21}$$

[i] Consult Appendix 2.

This NIG process $(X_{t\in[0,\infty)})$ with the Lévy triplet $(A_X = 0, \ell_X, \gamma_X)$ defined on a filtered probability space $(\Omega, \mathcal{F}_{t\in[0,\infty]}, \mathbb{P})$ possesses the following properties. It is a pure jump Lévy process (i.e. a purely non-Gaussian Lévy process) which is equivalent to stating that the Gaussian variance term is zero $A_X = 0$ following the Lévy-Itô decomposition of the sample paths. Its characteristic function can be obtained by the use of the subordination theorem of Lévy processes of the equation (6). The characteristic exponent of the Brownian motion with drift is:

$$\psi_W(\omega) = i\beta\omega - \frac{\omega^2}{2}. \tag{22}$$

Substitution of (22) and (20) into (6) after the consideration of the drift μ produces:

$$\phi_{NIG,X}(\omega;\alpha,\beta,\mu,\delta) = \exp\left[i\omega\mu t + t\delta\left\{\sqrt{\alpha^2-\beta^2} - \sqrt{\alpha^2-(\beta+i\omega)^2}\right\}\right]. \tag{23}$$

Its probability density is given by:

$$\mathbb{P}_{NIG}(x_t;\alpha,\beta,\mu,\delta)$$

$$= \frac{\alpha}{\pi}\exp\left(\delta t\sqrt{\alpha^2-\beta^2}\right)\exp\left\{\beta(x_t-\mu t)\right\}\frac{K_1\left(\alpha\delta t\sqrt{1+\left(\frac{x_t-\mu t}{\delta t}\right)^2}\right)}{\sqrt{1+\left(\frac{x_t-\mu t}{\delta t}\right)^2}}, \tag{24}$$

where K is the modified Bessel function of the second kind. The domain of the parameters are $\alpha \in \mathbb{R}^+$, $\beta \in \mathbb{R}$, $\mu \in \mathbb{R}$, $\delta \in \mathbb{R}^+$ and $\gamma \equiv \sqrt{\alpha^2-\beta^2} \in \mathbb{R}^+$. Note that this probability density can be easily computed using the conditionally normal property of the NIG process[j]:

[j] Of course, the adjustment for the drift μ is necessary.

$$\mathbb{P}_{NIG}(x_t;\alpha,\beta,\mu,\delta)=\int_0^\infty NIG(x_t\,|t=z_t=z)\mathbb{P}_{IG}(z_t;\delta,\gamma)dz$$

$$\mathbb{P}_{NIG}(x_t;\alpha,\beta,\mu,\delta)=\int_0^\infty \frac{1}{\sqrt{2\pi z}}\exp\left\{-\frac{(x_t-\beta z)^2}{2z}\right\}\frac{\delta t z_t^{-3/2}}{\sqrt{2\pi}}\exp\left\{\delta\gamma t-\frac{\left(\gamma^2 z_t+\delta^2 t^2 z_t^{-1}\right)}{2}\right\}dz\,.$$

Its standardized moments are computed by:

(25)
$$E[X_t]=\left(\mu+\frac{\beta\delta}{\sqrt{\alpha^2-\beta^2}}\right)t\,,$$

$$Variance[X_t]=\frac{\alpha^2\delta t}{\left(\sqrt{\alpha^2-\beta^2}\right)^3}\,,$$

$$Skewness[X_t]=\frac{3\beta}{\alpha\sqrt{\delta t}(\alpha^2-\beta^2)^{1/4}}\,,$$

$$Excess\ Kurtosis[X_t]=\frac{3\left(\alpha^2+4\beta^2\right)}{\alpha^2\delta t\sqrt{\alpha^2-\beta^2}}\,.$$

These standardized moments indicate that $\alpha\in\mathbb{R}^+$ is a shape parameter[k], $\beta\in\mathbb{R}$ is a skewnesss parameter, $\mu\in\mathbb{R}$ is a location parameter, and $\delta\in\mathbb{R}^+$ is an excess kurtosis parameter[l] of the probability density of the NIG process.

The Lévy measure of the NIG process is of the form:

(26)
$$\ell_{NIG,X}(x;\alpha,\beta,\delta)=\frac{\alpha\delta}{\pi}\frac{\exp(\beta x)}{|x|}K_1\left(\alpha|x|\right).$$

which has the infinite total mass:

$$\int_{-\infty}^{\infty}\ell_{NIG,X}(x)dx=\infty\,.$$

[k] The larger α leads to the smaller variance of the density.

[l] The smaller δ leads to the higher excess kurtosis (fatter tailed and higher peaked) of the density.

In other words, the NIG process is an infinite activity Lévy process which means that the NIG process has infinitely many small jumps and a finite number of large jumps inheriting the infinite arrival rate of jumps from the IG subordinator. The NIG process is also a Lévy process of infinite variation in the interval $[0,\infty)$. In other words, it is a Lévy process satisfying:

$$\int_{|x|<1} |x| \ell_{NIG,X}(x)dx = \infty .$$

Consult theorem 3.11 of Matsuda (2005a). Examples of the Lévy measure of the NIG process (26) are plotted in Figure 2. The sign of $\beta \in \mathbb{R}$ determines the skewness of the NIG Lévy measure as illustrated by Panel A. Larger values of $\alpha \in \mathbb{R}^+$ lead to the smaller overall arrival rate of the NIG Lévy measure as shown by Panel B. Larger values of $\delta \in \mathbb{R}^+$ make the overall arrival rate of jumps larger as depicted by Panel C.

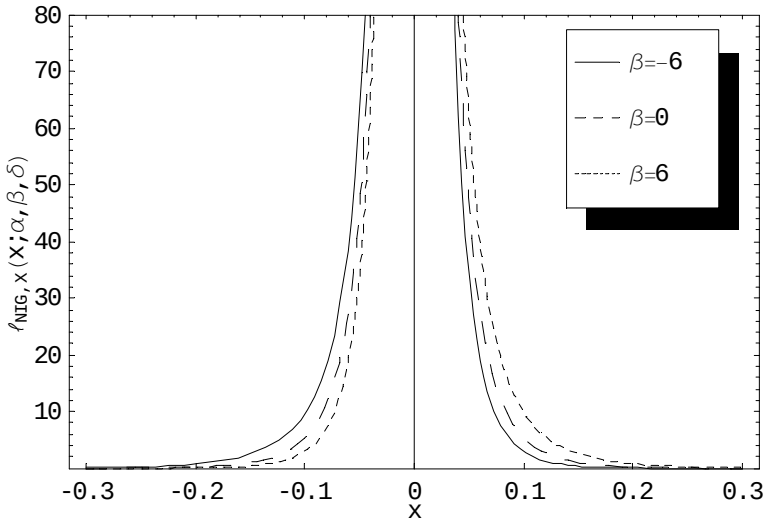

A) Lévy measure of NIG process with various values for β Parameters fixed are $\alpha = 20$ and $\delta = 0.6$.

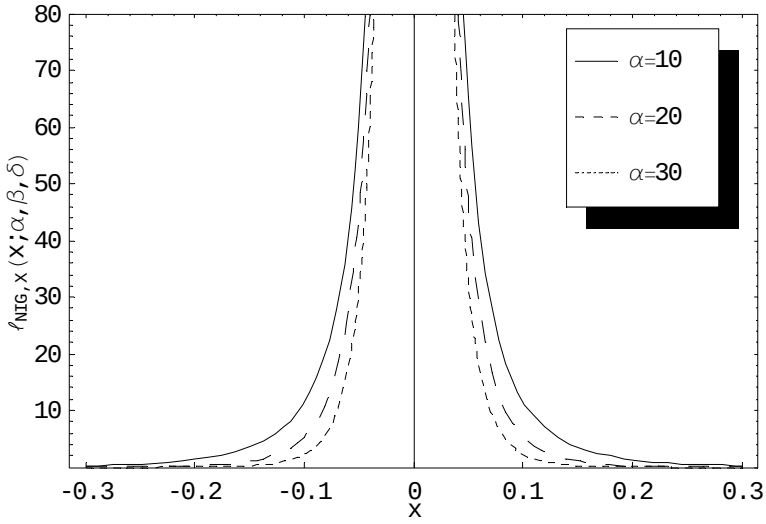

B) Lévy measure of NIG process with various values for α Parameters fixed are $\beta = 0$ and $\delta = 0.6$.

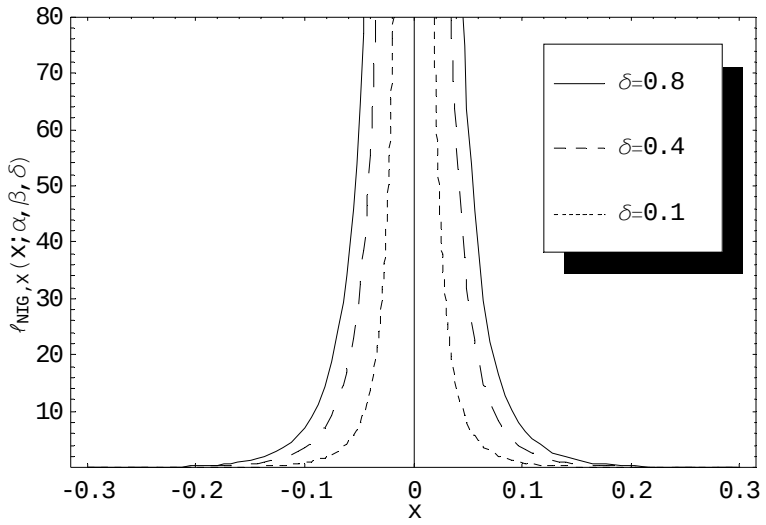

C) Lévy measure of NIG process with various values for δ Parameters fixed are $\alpha = 20$ and $\beta = 0$.

Figure 2 Plot of Lévy measure $\ell_{NIG,X}(x;\alpha,\beta,\delta)$ of NIG process

The NIG model specifies the asset price dynamics $(S_{t\in[0,T]})$ defined on a filtered risk neutral probability space $(\Omega, \mathcal{F}_{t\in[0,T]}, \mathbb{Q})$ as an exponential (geometric) of a Lévy process $(L_{t\in[0,T]})$:

$$S_t = S_0 \exp(L_t),$$

where the choice of the Lévy process is the NIG process plus the drift $r - \varpi_{VG,\mathbb{Q}}$:

(27) $$L_t \equiv (r - \varpi_{NIG,\mathbb{Q}})t + NIG(x_t; \alpha_{\mathbb{Q}}, \beta_{\mathbb{Q}}, \mu_{\mathbb{Q}}, \delta_{\mathbb{Q}}),$$

where $r \in \mathbb{R}^+$ is the instantaneous risk-free interest rate and all parameters are under the risk neutral probability measure $\mathbb{Q}$. The term $\varpi_{NIG,\mathbb{Q}}$ is the convexity correction which takes the following form in the NIG model:

(28) $$\varpi_{NIG,\mathbb{Q}} \equiv \mu_{\mathbb{Q}} + \delta_{\mathbb{Q}}\sqrt{\alpha_{\mathbb{Q}}{}^2 - \beta_{\mathbb{Q}}{}^2} - \delta_{\mathbb{Q}}\sqrt{\alpha_{\mathbb{Q}}{}^2 - \left(\beta_{\mathbb{Q}} + 1\right)^2}.$$

Note that this form of the convexity correction (28) necessitates one additional restriction on the parameters:

(29) $$\alpha^2 - \left(\beta + 1\right)^2 \in \mathbb{R}^+.$$

From the equation (27) and the definition (14) of the log return, we have the following relationship:

(30) $$x_t = R_t - (r - \varpi_{NIG,\mathbb{Q}})t.$$

Thus, the probability density of the log return in the NIG model under the risk neutral probability measure $\mathbb{Q}$ can be expressed using the density (24) as:

$$\mathbb{Q}_{NIG}(R_t; \alpha, \beta, \mu, \delta)$$

(31) $$= \frac{\alpha}{\pi}\exp\left(\delta t\sqrt{\alpha^2 - \beta^2}\right)\exp\left\{\beta\left(x_t - \mu t\right)\right\}\frac{K_1\left(\alpha\delta t\sqrt{1 + \left(\frac{x_t - \mu t}{\delta t}\right)^2}\right)}{\sqrt{1 + \left(\frac{x_t - \mu t}{\delta t}\right)^2}},$$

with the equation (30). Note that all parameters in the density (31) are under the risk neutral probability measure $\mathbb{Q}$.

2.C CGMY Model by Carr, Geman, Madan, and Yor (2002)

Koponen (1995) in the field of physics originally proposed a class of Lévy processes called tempered stable processes under the name of truncated Lévy flights. CGMY process is a subclass of tempered stable processes.[m]

Consider a fixed filtered probability space $(\Omega, \mathcal{F}_{t\in[0,\infty)}, \mathbb{P})$. The CGMY process $(X_{t\in[0,\infty)})$ is defined as a Lévy process with the Lévy triplet $(A_X = 0, \ell_X, \gamma_X = 0)$ whose Lévy measure is given by:

$$\ell_{CGMY,X}(x; C, G, M, Y) = \frac{C\exp(-G|x|)}{|x|^{1+Y}} 1_{x<0} + \frac{C\exp(-Mx)}{x^{1+Y}} 1_{x>0}, \tag{32}$$

where $C \in \mathbb{R}^+$, $G \in \mathbb{R}^+$, $M \in \mathbb{R}^+$, and $Y < 2$[n]. Examples of the Lévy measure of the CGMY process (32) are plotted in Figure 3. The overall arrival rate of jumps is controlled by the parameter C indicating that the larger values of C result in the larger overall arrival rate of jumps as shown by Panel A. Panel B depicts the role of the parameters G and M which are the exponential decay rates of the lower and upper tails of the Lévy measure, respectively. When $G = M$, the Lévy measure is symmetric. When $G < M$, the upper tail of the Lévy measure is decayed more and the lower tail of the Lévy measure is heavier which indicates that the arrival rate of negative jumps is higher than that of large jumps. The most interesting parameter is Y since it controls the activity rate (i.e. total mass) of the Lévy measure and the variation of the CGMY process. Y also determines whether the Lévy measure is a monotonically decreasing function of the jump size $|x|$.

[m] Consult section 4.5 and remark 4.4 of Cont and Tankov (2004).

[n] The condition $Y < 2$ ensures the integrability of the Lévy measure with respect to x^2 in the neighborhood of zero.

Table 1 summarizes the role of the parameter Y which is based on the Table 1 of CGMY (2002) and Panel C and D of Figure 3 illustrates the role of Y .

Table 1 Role of parameter Y (Based on the Table 1 of CGMY (2002).)

Y	Lévy measure $\ell_{CGMY,X}(x)$		Variation of the process
	monotonically decreasing	total mass $\int_{-\infty}^{\infty} \ell_{CGMY,X}(x)dx$	
$Y<-1$	no	finite	finite
$-1<Y<0$	yes	finite	finite
$0<Y<1$	yes	infinite	finite
$1<Y<2$	yes	infinite	infinite

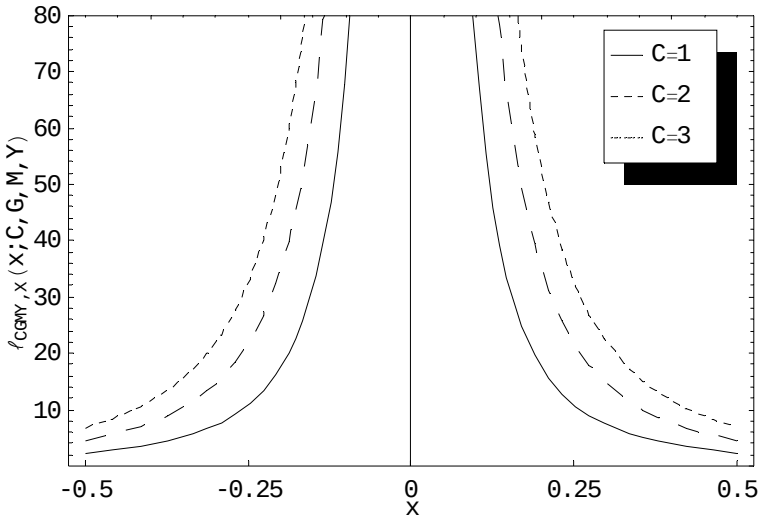

A) Lévy measure of CGMY process with various values for C Parameters fixed are $G=1,\ M=1$, and $Y=0.9$.

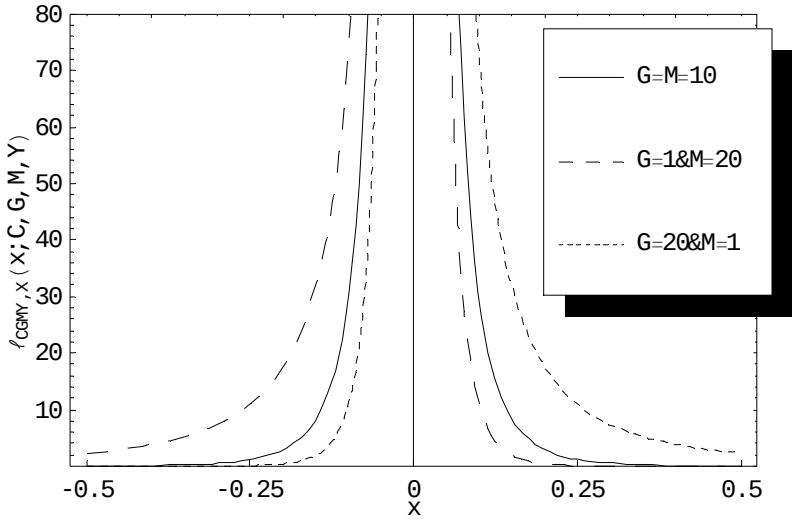

B) Lévy measure of CGMY process with various values for G and M Parameters fixed are $C = 1$ and $Y = 0.9$.

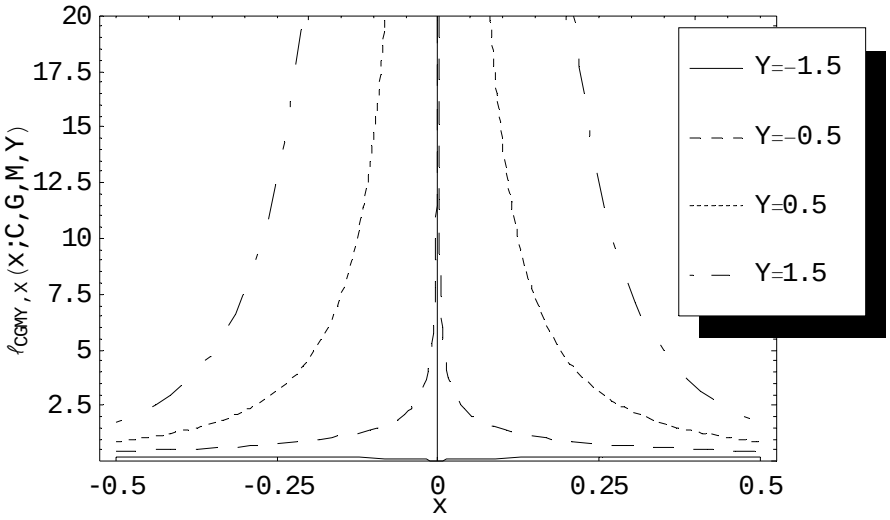

C) Lévy measure of CGMY process with various values for Y Parameters fixed are $C = 0.5$, $G = 1$, and $M = 1$.

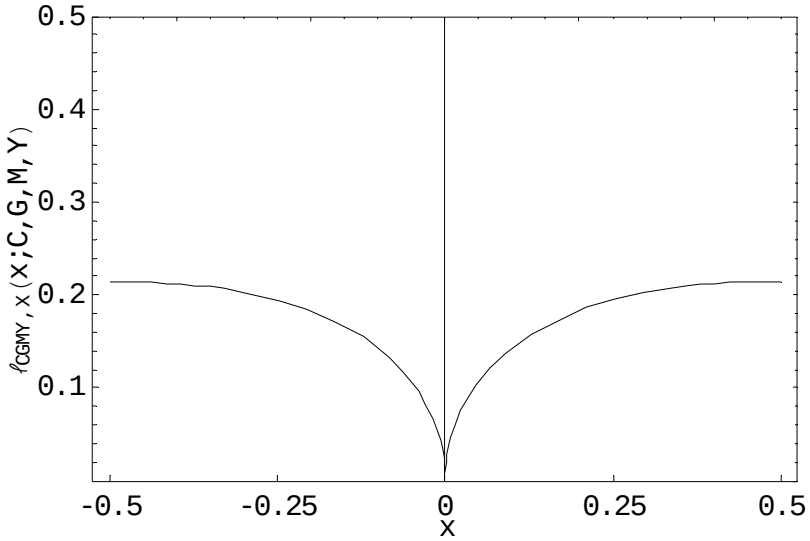

D) Lévy measure of CGMY process with $Y = -1.5$ Parameters fixed are $C = 0.5$, $G = 1$, and $M = 1$.

Figure 3 Plot of Lévy measure $\ell_{CGMY,X}(x;C,G,M,Y)$ of CGMY process

This CGMY process $(X_{t\in[0,\infty)})$ with the Lévy triplet $(A_X = 0, \ell_X, \gamma_X = 0)$ defined on a filtered probability space $(\Omega, \mathcal{F}_{t\in[0,\infty]}, \mathbb{P})$ possesses the following properties. It is a pure jump Lévy process (i.e. a purely non-Gaussian Lévy process) which is equivalent to stating that the Gaussian variance term is zero $A_Y = 0$ following the Lévy-Itô decomposition of the sample paths. Its characteristic function can be obtained by the use of the Lévy-Khinchin representation without truncation of large jumps[o]:

$$\phi_X(\omega) = \exp\left(t\psi_X(\omega)\right),$$

where $\psi_X(\omega)$ is the characteristic exponent of the CGMY process:

(33) $$\psi_X(\omega) = \int_{-\infty}^{\infty} \left\{\exp(i\omega x) - 1 - i\omega x\right\} \ell_{CGMY,X}(x;C,G,M,Y)dx .$$

Following Cont and Tankov (2004), the characteristic exponent of the CGMY process is calculated as:

[o] Consult Appendix 3.

(34) $\psi_{CGMY,X}(\omega;C,G,M,Y)$

$$= CG^{Y}\Gamma(-Y)\left\{\left(1+\frac{i\omega}{G}\right)^{Y}-1-\frac{i\omega Y}{G}\right\}+CM^{Y}\Gamma(-Y)\left\{\left(1-\frac{i\omega}{M}\right)^{Y}-1+\frac{i\omega Y}{M}\right\}.$$

In the general case, the probability density function of the CGMY process is not available in closed form. Its standardized moments are computed by:

(35) $$E[X_t]=\gamma_X t=0,$$

$$Variance[X_t]=tC\Gamma(2-Y)\left(G^{Y-2}+M^{Y-2}\right),$$

$$Skewness[X_t]=\frac{tC\Gamma(3-Y)\left(-G^{Y-3}+M^{Y-3}\right)}{\left(Variance[X_t]\right)^{3/2}},$$

$$Excess\ Kurtosis[X_t]=\frac{tC\Gamma(4-Y)\left(G^{Y-4}+M^{Y-4}\right)}{\left(Variance[X_t]\right)^{2}}.$$

The VG process can be obtained as a special case of the CGMY process when:

$$C=1/\nu,$$

$$G=\frac{1}{\sqrt{\frac{\theta^2\nu^2}{4}+\frac{\sigma^2\nu}{2}}-\frac{\theta\nu}{2}},$$

$$M=\frac{1}{\sqrt{\frac{\theta^2\nu^2}{4}+\frac{\sigma^2\nu}{2}}+\frac{\theta\nu}{2}},$$

$$Y=0.$$

The CGMY model specifies the asset price dynamics $(S_{t\in[0,T]})$ defined on a filtered risk neutral probability space $(\Omega,\mathcal{F}_{t\in[0,T]},\mathbb{Q})$ as an exponential (geometric) of a Lévy process $(L_{t\in[0,T]})$:

$$S_t = S_0 \exp(L_t),$$

where the choice of the Lévy process is the CGMY process plus the drift $r - \varpi_{CGMY,\mathbb{Q}}$:

(36) $$L_t \equiv (r - \varpi_{CGMY,\mathbb{Q}})t + CGMY(x_t; C_{\mathbb{Q}}, G_{\mathbb{Q}}, M_{\mathbb{Q}}, Y_{\mathbb{Q}}),$$

where $r \in \mathbb{R}^+$ is the instantaneous risk-free interest rate and all parameters are under the risk neutral probability measure $\mathbb{Q}$. The term $\varpi_{CGMY,\mathbb{Q}}$ is the convexity correction which takes the following form in the CGMY model:

(37) $$\varpi_{CGMY,\mathbb{Q}} = C_{\mathbb{Q}} G_{\mathbb{Q}}{}^{Y_{\mathbb{Q}}} \Gamma(-Y_{\mathbb{Q}}) \left\{ \left(1 + \frac{1}{G_{\mathbb{Q}}} \right)^{Y_{\mathbb{Q}}} - 1 - \frac{Y_{\mathbb{Q}}}{G_{\mathbb{Q}}} \right\}$$

$$+ C_{\mathbb{Q}} M_{\mathbb{Q}}{}^{Y_{\mathbb{Q}}} \Gamma(-Y_{\mathbb{Q}}) \left\{ \left(1 - \frac{1}{M_{\mathbb{Q}}} \right)^{Y_{\mathbb{Q}}} - 1 + \frac{Y_{\mathbb{Q}}}{M_{\mathbb{Q}}} \right\}.$$

Defining the log return as $R_t \equiv \ln(S_t / S_0)$, we have the following relationship from the equation (36):

(38) $$x_t = R_t - (r - \varpi_{CGMY,\mathbb{Q}})t.$$

3. Traditional Lévy Models

In this section, we present two non-pure jump Lévy models in which the asset price dynamics is modeled using the Gaussian Lévy process and the non-Gaussian Lévy process. Intuitively, non-pure jump Lévy processes contain a Brownian motion which is equivalent to stating that the Gaussian variance term A_X is not zero following Lévy-Itô decomposition of the sample paths. The classic Black-Scholes model (1973) is the only continuous (i.e. Gaussian) Lévy model in which the asset price dynamics is modeled by the Brownian motion. Another classic Merton jump diffusion model (1976) is the non-Gaussian Lévy model in which the asset price dynamics is modeled by the jump diffusion process which possesses the discontinuities. Consult Matsuda (2005a) for the detailed treatment of the mathematics of traditional Lévy processes.

3.A Black-Scholes Model (1973)

Let $(B_{t\in[0,\infty)})$ be a standard Brownian motion defined on a filtered probability space $(\Omega, \mathcal{F}_{t\in[0,\infty)}, \mathbb{P})$ with the Lévy triplet $(A_B = 1, \ell_B = 0, \gamma_B = 0)$. Define a multiplicative Brownian motion as $(X_{t\in[0,\infty)}) \equiv (\sigma B_{t\in[0,\infty)})$ with the Lévy triplet $(A_X = \sigma^2, \ell_X = 0, \gamma_X = 0)$. A multiplicative Brownian motion $(X_{t\in[0,\infty)})$ or a Brownian motion in general is the only continuous Lévy process which is equivalent to the Gaussian Lévy process. Its characteristic function can be obtained by the use of the general Lévy-Khinchin representation[p]:

$$\phi_X(\omega) = \exp\left(-\frac{\sigma^2 t\omega^2}{2}\right). \tag{39}$$

Its probability density is given by:

[p] Consult Appendix 3.

(40) $$\mathbb{P}_X(x_t) = \frac{1}{\sqrt{2\pi\sigma^2 t}} \exp\left(-\frac{x_t^2}{2\sigma^2 t}\right),$$

where $\sigma \in \mathbb{R}^+$ is a shape parameter.

The Lévy measure of the Brownian motion is zero because it is a stochastic process with continuous sample paths (i.e. no jumps):

(41) $$\ell_X(x) = 0 .$$

A Brownian motion is also a Lévy process of infinite variation in the interval $[0, \infty)$.

The BS model specifies the asset price dynamics $(S_{t\in[0,T]})$ defined on a filtered risk neutral probability space $(\Omega, \mathcal{F}_{t\in[0,T]}, \mathbb{Q})$ as an exponential of a Lévy process $(L_{t\in[0,T]})$:

$$S_t = S_0 \exp(L_t),$$

where the choice of the Lévy process is the multiplicative Brownian motion plus the drift $r - \varpi_{BS,\mathbb{Q}}$:

(42) $$L_t \equiv (r - \varpi_{BS,\mathbb{Q}})t + X(x_t; \sigma_{\mathbb{Q}}),$$

where $r \in \mathbb{R}^+$ is the instantaneous risk-free interest rate and all parameters are under the risk neutral probability measure $\mathbb{Q}$. The term $\varpi_{BS,\mathbb{Q}}$ is the convexity correction which takes the following form in the BS model:

(43) $$\varpi_{BS,\mathbb{Q}} \equiv \frac{\sigma_{\mathbb{Q}}^2}{2}.$$

Defining the log return (i.e. log price relative) of the asset price as $R_t \equiv \ln(S_t / S_0)$ and using the equation (42):

(44) $$x_t = R_t - (r - \varpi_{BS,\mathbb{Q}})t .$$

Since obviously the drift $r-\varpi_{BS,\mathbb{Q}}$ is deterministic, the probability density of the log return in the BS model under the risk neutral probability measure $\mathbb{Q}$ can be expressed using the probability density (40) and the relationship (44) as:

$$\mathbb{Q}_{BS}(R_t;\sigma)=\frac{1}{\sqrt{2\pi\sigma^2 t}}\exp\left[-\frac{\left\{R_t-\left(r-\varpi_{BS,\mathbb{Q}}\right)t\right\}^2}{2\sigma^2 t}\right]. \tag{45}$$

3.B Merton Jump Diffusion Model (1976)

Consider a fixed filtered probability space $(\Omega,\mathcal{F}_{t\in[0,\infty]},\mathbb{P})$. A jump diffusion process $(X_{t\in[0,\infty]})$ with the Lévy triplet $(A_X=\sigma^2,\ell_X=\lambda f(x),\gamma_X=0)$ is defined as a Brownian motion plus a compound Poisson process:

$$(X_{t\in[0,\infty]})\equiv(\sigma B_{t\in[0,\infty]})+\sum_{i=1}^{N_t}X_i\,, \tag{46}$$

where $(\sigma B_{t\in[0,\infty]})$ is a multiplicative Brownian motion with the Lévy triplet $(A_B=\sigma^2,\ell_B=0,\gamma_B=0)$, $\sum_{i=1}^{N_t}X_i$ is a compound Poisson process with the Lévy triplet $(A_C=0,\ell_C=\lambda f(x),\gamma_C=0)$ which is the sum of *i.i.d.* jumps X_i from the jump size probability density $f(x)$, and $(N_{t\in[0,\infty]})$ is a Poisson process with the intensity $\lambda\in\mathbb{R}^+$ which counts the number of random arrival times T_k of an event in the time interval $[0,t]$:

$$N_t=\sum_{k\geq 1}1_{t\geq T_k}\,. \tag{47}$$

Note that a Poisson process $(N_{t\in[0,\infty]})$ and the jumps sizes $(X_i)_{i\geq 1}$ are assumed to be independent. This jump diffusion process $(X_{t\in[0,\infty]})$ possesses the following properties. It is a non-Gaussian Lévy process (also called a jump Lévy process), but not a pure jump Lévy process (also called a purely non-Gaussian Lévy process) because the Gaussian

variance term of the jump diffusion process A_X is non-zero. In other words, $A_X = \sigma^2 \neq 0$ indicates that the process contains a Brownian motion[q]. The Lévy measure of the jump diffusion process is given by:

(48) $$\ell_{JD,X}(x;\lambda) = \lambda f(x),$$

where $f(x)$ is the jump size probability density. The total mass of the Lévy measure of the jump diffusion process is the intensity parameter λ because a Lévy measure $\ell(x)$ measures the arrival rate of jumps:

$$\int_{-\infty}^{\infty} \ell_{JD,X}(x)dx = \int_{-\infty}^{\infty} \lambda f(x)dx = \lambda \int_{-\infty}^{\infty} f(x)dx = \lambda < \infty,$$

which is finite because the number of arrivals of an event is almost surely finite for any $t > 0$ including an infinite time horizon $t = \infty$[r]. In other words, the jump diffusion process is a finite activity Lévy process which means that the process has finite number of small jumps and finite number of large jumps. The jump diffusion process is also a Lévy process of infinite variation in the interval $[0,\infty)$ because $A_X = \sigma^2 \neq 0$.[s] Merton jump diffusion (MJD) model specifies the log return jump size density as the normal, i.e. $X_i \sim i.i.d.\ Normal(\mu, \delta^2)$:

(49) $$f_{MJD}(x) = \frac{1}{\sqrt{2\pi\delta^2}} \exp\left\{-\frac{(x-\mu)^2}{2\delta^2}\right\}.$$

Thus, the Lévy measure in MJD model can be expressed as:

[q] Consult section 3.7.1 of Matsuda (2005a).

[r] The number (6) of theorem 4.10 of Matsuda (2005a).

[s] Consult theorem 3.11 of Matsuda (2005a).

(50) $$\ell_{MJD,X}(x;\lambda,\mu,\delta)=\frac{\lambda}{\sqrt{2\pi\delta^2}}\exp\left\{-\frac{(x-\mu)^2}{2\delta^2}\right\}.$$

Figure 4 plots the examples of the Lévy measure of the MJD process (50). The overall arrival rate of jumps is controlled by the intensity parameter λ indicating that the larger values of λ result in the larger overall arrival rate of jumps. The parameter $\mu \in \mathbb{R}$ controls the location of the Lévy measure and the parameter $\delta \in \mathbb{R}^+$ controls its shape. Apparently, the MJD Lévy measure is always symmetric.

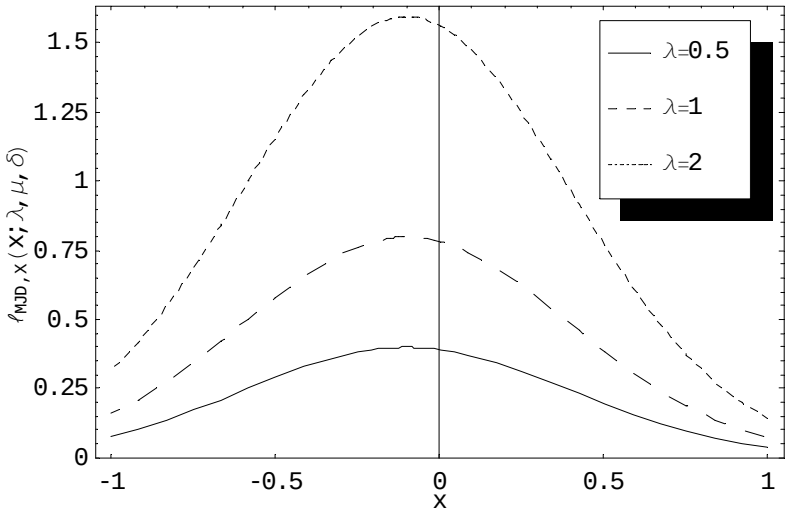

Figure 4 Plot of Lévy measure $\ell_{MJD,X}(x;\lambda,\mu,\delta)$ of MJD process with various values for λ Parameters fixed are $\mu=-0.1$ and $\delta=0.5$.

The characteristic function of MJD process can be obtained by the use of the Lévy-Khinchin representation[t] as:

(51) $$\phi_{MJD,X}(\omega;\sigma,\lambda,\mu,\delta)=\exp\left[t\left\{-\frac{\sigma^2\omega^2}{2}+\lambda\left(\phi_f(\omega)-1\right)\right\}\right],$$

[t] Consult the section 4.3.4 of Matsuda (2005a) where the characteristic function of a compound Poisson process is obtained by using the Lévy-Khinchin representation for the finite variation processes.

where ϕ_f is the characteristic function of the jump size density:

$$\phi_f(\omega) = \exp\left(i\omega\mu - \frac{\delta^2\omega^2}{2} \right).$$

The probability density of the MJD process can be computed using the conditionally normal property of the jump diffusion process of the equation (46)[u]:

$$\mathbb{P}_{MJD}(x_t;\sigma,\lambda,\mu,\delta) = \sum_{j=0}^{\infty} \mathbb{P}(x_t \,|\, N_t = j)\mathbb{P}_{Poisson}(N_t = j)$$

$$\text{(52)} \qquad \mathbb{P}_{MJD}(x_t;\sigma,\lambda,\mu,\delta) = \sum_{j=0}^{\infty} \frac{e^{-\lambda t}(\lambda t)^j}{j!} \frac{1}{\sqrt{2\pi\left(\sigma^2 t + j\delta^2\right)}} \exp\left\{ -\frac{\left(x_t - j\mu\right)^2}{2\left(\sigma^2 t + j\delta^2\right)} \right\}.$$

Its standardized moments are computed by:

$$\text{(53)} \qquad E[X_t] = \lambda t\mu,$$

$$Variance[X_t] = (\sigma^2 + \lambda\delta^2 + \lambda\mu^2)t,$$

$$Skewness[X_t] = \frac{t\lambda\mu(\mu^2 + 3\delta^2)}{Variance[X_t]^{3/2}},$$

$$Excess\ Kurtosis[X_t] = \frac{t\lambda(\mu^4 + 3\delta^4 + 6\mu^2\delta^2)}{Variance[X_t]^2}.$$

These standardized moments indicate that μ is a skewness parameter with $\mu = 0$ producing the symmetric probability density. Larger values for λ and σ lead to the larger variance and smaller excess kurtosis of the probability density.

MJD model specifies the asset price dynamics $(S_{t\in[0,T]})$ defined on a filtered risk neutral probability space $(\Omega, \mathcal{F}_{t\in[0,T]}, \mathbb{Q})$ as an exponential of a Lévy process $(L_{t\in[0,T]})$:

[u] This computation involves the series expansion rather than the integration because a compound Poisson process is a continuous time stochastic process with the discontinuous sample paths.

$$S_t = S_0 \exp(L_t),$$

where the choice of the Lévy process is the jump diffusion process plus the drift $r - \varpi_{MJD,\mathbb{Q}}$:

$$L_t \equiv (r - \varpi_{MJD,\mathbb{Q}})t + MJD(x_t; \sigma_{\mathbb{Q}}, \lambda_{\mathbb{Q}}, \mu_{\mathbb{Q}}, \delta_{\mathbb{Q}}), \tag{54}$$

where $r \in \mathbb{R}^+$ is the instantaneous risk-free interest rate and all parameters are under the risk neutral probability measure $\mathbb{Q}$. The term $\varpi_{MJD,\mathbb{Q}}$ is the convexity correction which takes the following form in the MJD model:

$$\varpi_{MJD,\mathbb{Q}} = \lambda_{\mathbb{Q}} \left\{ \exp\left(\mu_{\mathbb{Q}} + \frac{\delta_{\mathbb{Q}}^{\,2}}{2} \right) - 1 \right\} + \frac{\sigma_{\mathbb{Q}}^{\,2}}{2}. \tag{55}$$

Defining the log return (i.e. log price relative) of the asset price as $R_t \equiv \ln(S_t / S_0)$ and using the equation (54):

$$x_t = R_t - (r - \varpi_{MJD,\mathbb{Q}})t. \tag{56}$$

Since obviously the drift $r - \varpi_{MJD,\mathbb{Q}}$ is deterministic, the probability density of the log return in the MJD model under the risk neutral probability measure $\mathbb{Q}$ can be expressed using the probability density (52) and the relationship (56) as:

$$\mathbb{Q}_{MJD}(R_t; \sigma, \lambda, \mu, \delta) = \sum_{j=0}^{\infty} \frac{e^{-\lambda t}(\lambda t)^j}{j!} \frac{1}{\sqrt{2\pi\left(\sigma^2 t + j\delta^2\right)}} \exp\left\{ -\frac{\left(x_t - j\mu\right)^2}{2\left(\sigma^2 t + j\delta^2\right)} \right\}, \tag{57}$$

with the equation (56). Note that all parameters in the density (57) are under the risk neutral probability measure $\mathbb{Q}$.

Table 2 summarizes all the models described thus far.

Table 2 Model Comparison

Model	Sample Paths Property	Total mass of Lévy measure $\int_{-\infty}^{\infty} \ell_X(x)dx$	Variation of the process
BS	continuous	0	infinite
MJD	continuous with occasional Jumps	finite and small	infinite
VG	purely discontinuous	∞	finite
NIG	purely discontinuous	∞	infinite
CGMY	purely discontinuous	$0 < \leq \infty$	finite or infinite

4. Calibration Methodology

4.A Data Description

Our data consist of daily settlement call option prices on S&P 500 futures with March 2005 maturity obtained from Chicago Mercantile Exchange (CME) Daily Bulletin for the sample period from March 24, 2004, through March 16, 2005[v] for the total of 248 trading days. These American style option prices are converted to European style option prices using Barone-Adesi and Whaley (1987) quadratic approximation method to adjust for the early exercise premium. After eliminating call prices less than 0.125 due to reliability issues, the data used consist of a total of 6567 call prices.

Daily series of three month Treasury Bill rate are used as appropriate risk-free interest rates.

4.B Introduction to Calibration

Two problems are said to be inverse to each other, if formulating one problem involves the other problem. One of these two problems (the simpler one or the older one) is called a direct problem and the other is called an inverse problem. The inverse problem which we deal with is called a parameter identification problem in which we try to identify physical parameters from observations of the evolution of the system. Let η be a vector of parameters to be identified. In our context, a direct problem is formulated as:

$$C_i^{\text{model}}(\hat{\eta}, S_t, K_i, T) = e^{-r(T-t)} E^{\mathbb{Q}}\left[\left(S_T - K_i\right)^+ \middle| \mathcal{F}_t\right], \tag{58}$$

where European option prices C_i^{model} across different strikes $K_{i\in I}$ are calculated given a vector of parameters $\hat{\eta}$ and variables such as strikes K_i and a maturity T. An inverse problem is formulated as the reverse of this procedure: Identify a vector of parameters η

[v] March 16, 2005 is one day before the last trading day.

under measure $\mathbb{Q}$ [w] such that the discounted asset price process $(e^{-rt}S_{t\in 0\le t\le T})$ becomes a martingale and which reproduce model option prices consistent with market observed option prices:

(59) $$C_i^{\text{model}}(S_t, K_i, T) = C_i^{\text{market}}.$$

Because market option prices $(C_{i\in I}^{\text{market}})$ include noise (i.e. bid-ask spreads), we need not to find a risk-neutral martingale measure $\mathbb{Q} \sim \mathbb{P}$ which exactly reproduces market observed prices. Thus, the practical solution for the calibration problem becomes a best approximation problem between market observed prices and model calibrated prices. In most literatures, this approximation is done in a least squares sense. Thus, a calibration problem can be expressed as a nonlinear least squares problem of the form:

(60) $$\eta^{\mathbb{Q}} = \arg\min_{\mathbb{Q}\in\wp} \sum_{i=1}^{N} \left| C_i^{\text{model}}(S_t, K_i, T) - C_i^{\text{market}} \right|^2,$$

where the implied risk neutral parameter vector $\eta^{\mathbb{Q}}$ is chosen by minimizing the sum of squared dollar pricing errors between market observed prices and model calibrated prices. Note that minimizing the sum of squared dollar pricing errors has the bias toward more expensive in-the-money options over relatively cheaper out-of-the-money options. But this is the standard objective function in the literature such as Dumas, Fleming and Whaley (1995), Bates (1996), Bakshi, Cao and Chen (1997), and Cont and Tankov (2004). Bakshi, Cao and Chen (1997) propose an alternative objective function which is to minimize the sum of squared percentage pricing errors:

$$\eta^{\mathbb{Q}} = \arg\min_{\mathbb{Q}\in\wp} \sum_{i=1}^{N} \left| \frac{C_i^{\text{model}}(S_t, K_i, T) - C_i^{\text{market}}}{C_i^{\text{market}}} \right|^2,$$

[w] Called an implied risk neutral measure.

which has the bias toward cheaper out-of-the-money options.

4.C Pricing Methodology for Lévy Models

We employ Carr and Madan's (1999) Fourier transform option pricing approach with the modified call price. For more details, consult the chapter 8 of Matsuda (2004b). The use of the Fourier transform option pricing is necessary for some Lévy models because their probability densities cannot always be expressed using special functions of mathematics or they are unknown. Therefore, Carr and Madan rewrite the option pricing function involving the probability density into the option pricing function involving the characteristic function because the characteristic function of the Lévy process is always available in a closed form.[x]

[x] There is one-to-one relationship between a probability density and a characteristic functions (i.e. through Fourier transform) and both of which uniquely determine a probability distribution.

5. Calibration, Implied Dynamics, and In-Sample Performance of Lévy Models

5.A Dynamics of Calibrated Parameters

Using the data and procedure described in the section 4, each model is separately calibrated for each day. Table 3 reports the daily average, the standard error, the minimum, and the maximum of the calibrated parameters of each model for the sample period. Time series of calibrated parameters for each model are plotted from the day 1 which is March 24, 2004, through day 248 which is March 16, 2005 in Figure 5. Note that we set the NIG model's μ equal to zero because this parameter is a location parameter which only affects the mean of the equation (25) and can be incorporated into the parameters $\alpha, \beta,$ and δ. We observe the followings.

As expected and illustrated by Panel A) of Figure 5, the BS model's volatility parameter σ declines as the maturity of the S&P 500 futures option nears because the uncertainty regarding the terminal price declines.

The daily average of MJD model's σ is 0.09544 and smaller in size compared to the BS σ which is 0.14437 since the MJD model attributes the volatility to other parameters λ, μ, and δ.[y] The daily average of the intensity parameter λ of the MJD model is 0.77742 which means that the jump occurs 0.77742 times per year on average for this sample. It is very interesting to note that λ tends to increase (i.e. higher frequency of jumps) as the maturity nears as illustrated by Panel B) of Figure 5 and this tendency seems to be true regardless of the sample. Bakshi, Cao, and Chen (1997) reports the same observation. The MJD model's mean log return jump size μ is -14.899% on average and it declines as the maturity nears for the sample. As previously mentioned, the

[y] Look at the equation (53).

negative value of μ indicates the natively skewed log return probability density function. The MJD model's standard deviation parameter δ of mean log return jump size is 0.09411 on average and it declines as the maturity nears for the sample indicating the less uncertainty regarding the jump size.

The VG model's drift parameter θ is -0.16798 on average and it indicates the natively skewed log return probability density function. Panel C) of Figure 5 depicts the declining trend for the volatility parameter of the subordinated Brownian motion σ and the variance rate parameter ν. This contributes to the declining negative skewness and excess kurtosis of the log return probability density function for the sample period.

The NIG model's skewness parameter α is -11.7309 on average and it indicates the natively skewed log return probability density function. Panel D) of Figure 5 shows the increasing trend for the shape parameter α (which leads to smaller volatility) and the excess kurtosis parameter δ (which leads to higher excess kurtosis). But later it will be shown that the increase in δ is dominated by the increase in α and the increase in size in β and as a result, the excess kurtosis of the log return probability density function declines as the maturity approaches for the sample.

The CGMY model's parameter C is 0.06675 on average and it declines dramatically as the maturity nears indicating the smaller overall arrival rate of jumps at the near maturity. As expected, the lower tail decay rate parameter G is 2.35246 on average and much smaller than the upper tail decay rate parameter M which is 262.805. Less decayed lower tail means the negative skewness of the log return probability density function. We also observe that the estimates of G and M become extremely volatile as the maturity nears in contrast to that of C. The parameter Y estimated is 1.19952 for the sample which

confirms the monotonically decreasing Lévy measure, the infinite total mass of the Lévy measure (i.e. the infinite arrival rate of jumps), and the fact that the underlying S&P 500 futures price process is a process of infinite variation according to Table 1. Closer examination reveals that the calibrated Y is above one (the process is infinite variation) for 71% (175/248) of the days. But the Panel E) of Figure 5 shows the definite pattern of the estimated Y being less than one for the long maturity options and being above one for the short maturity options. For this reason, we divide the entire sample period into three subperiods. The first subperiod is the long term to maturity which include days with greater than or equal to 180 days to maturity (day 1 through day 69), the second subperiod is the medium term to maturity which include days with greater than or equal to 60 but less than 180 days to maturity (day 70 through day 190), and the third subperiod is the short term to maturity which include days with less than 60 days to maturity (day 191 through day 248). Interestingly, for the long term to maturity, the estimated Y is less than one (the underlying process is finite variation) for 68% of the period with the sub-mean 0.941. For the medium term to maturity, the estimated Y is above one for 78.5% of the period with the sub-mean 1.14. And for the short term to maturity, the estimated Y is above one for 100% of the period with the sub-mean 1.63. Thus, the underlying S&P 500 futures price shifted from the finite variation stochastic process to infinite variation stochastic process as the maturity moves from the long to the short term at least for the sample used here.

Table 3
Calibrated Parameters

The daily average, the standard error, the minimum, and the maximum of the calibrated parameters for the sample period are presented. Note that we set NIG's μ equal to zero because this parameter is insensitive to the option price.

Parameters		Daily Average	Standard Error	Minimum	Maximum
BS	σ	0.14437	0.02253	0.09714	0.19339
MJD	σ	0.09544	0.00669	0.07470	0.11761
	λ	0.77742	0.59858	0.29551	5.66366
	μ	-0.14899	0.06361	-0.29654	-0.00985
	δ	0.09411	0.02968	0.02681	0.14922
VG	θ	-0.16798	0.03133	-0.36617	-0.10567
	σ	0.13503	0.01758	0.09363	0.16591
	ν	0.39608	0.23908	0.00802	0.89766
NIG	α	20.7408	12.7483	9.60631	89.6984
	β	-11.7309	3.71075	-30.0897	-6.87204
	μ	0	0	0	0
	δ	0.24832	0.11783	0.15429	1.01836
CGMY	C	0.06675	0.05032	0.00259	0.33387
	G	2.35246	0.96472	0.34914	7.63829
	M	262.805	990.01	18.4187	7314.23
	Y	1.19952	0.29492	0.56393	1.77157

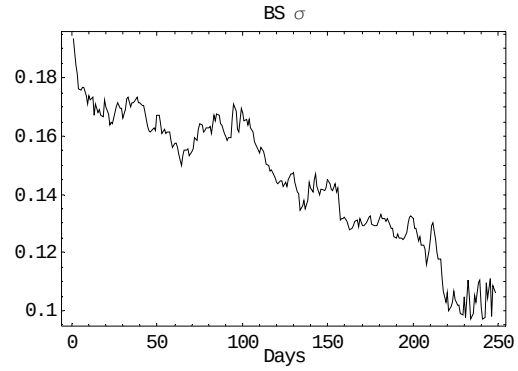

A) BS Model

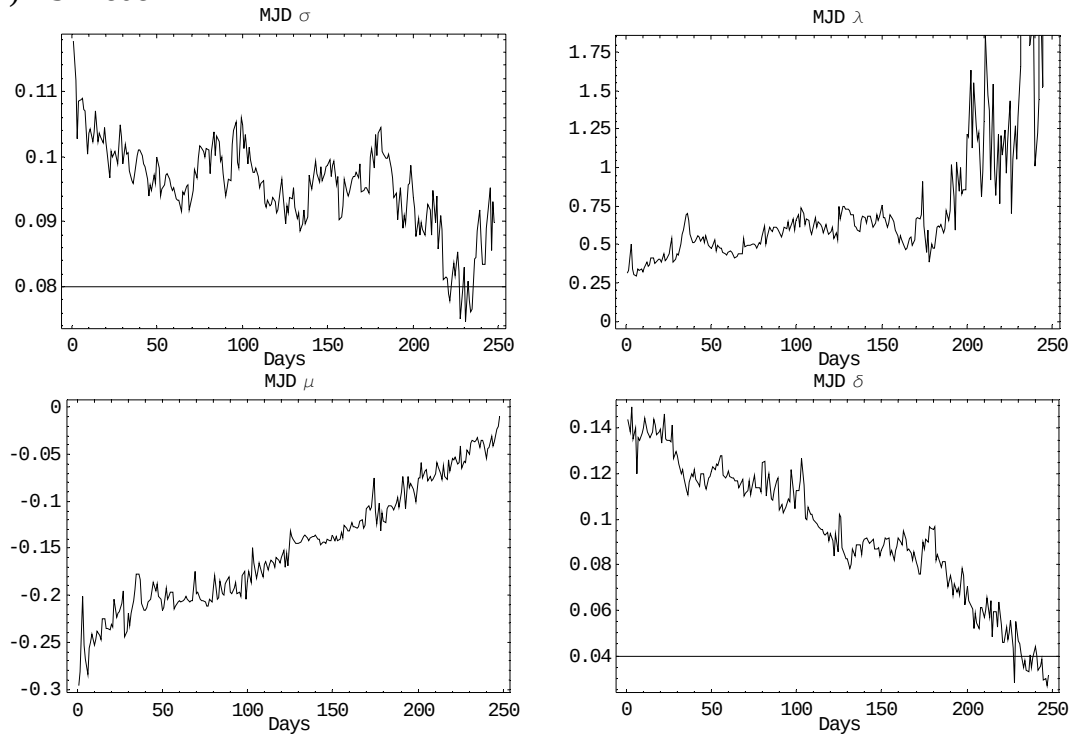

B) MJD Model

Figure 5 Dynamics of Calibrated Parameters Time series of calibrated parameters for each model are plotted from the day 1 which is March 24, 2004, through day 248 which is March 16, 2005.

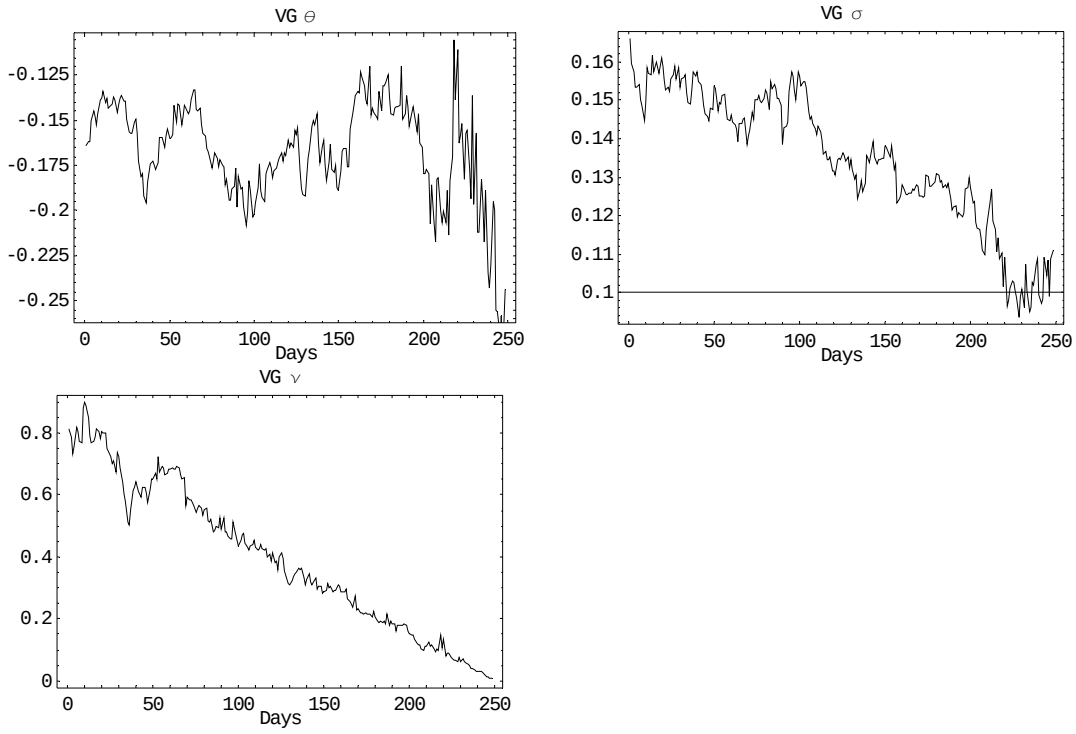

C) VG Model

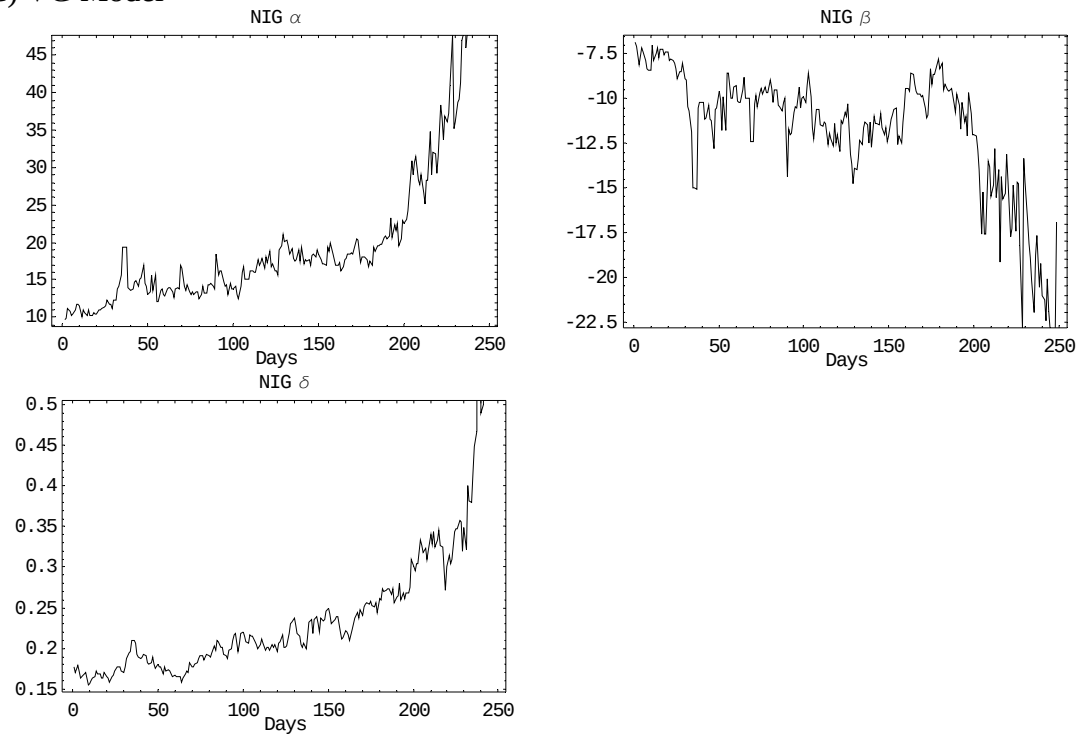

D) NIG Model

Figure 5 Dynamics of Calibrated Parameters (Continued)

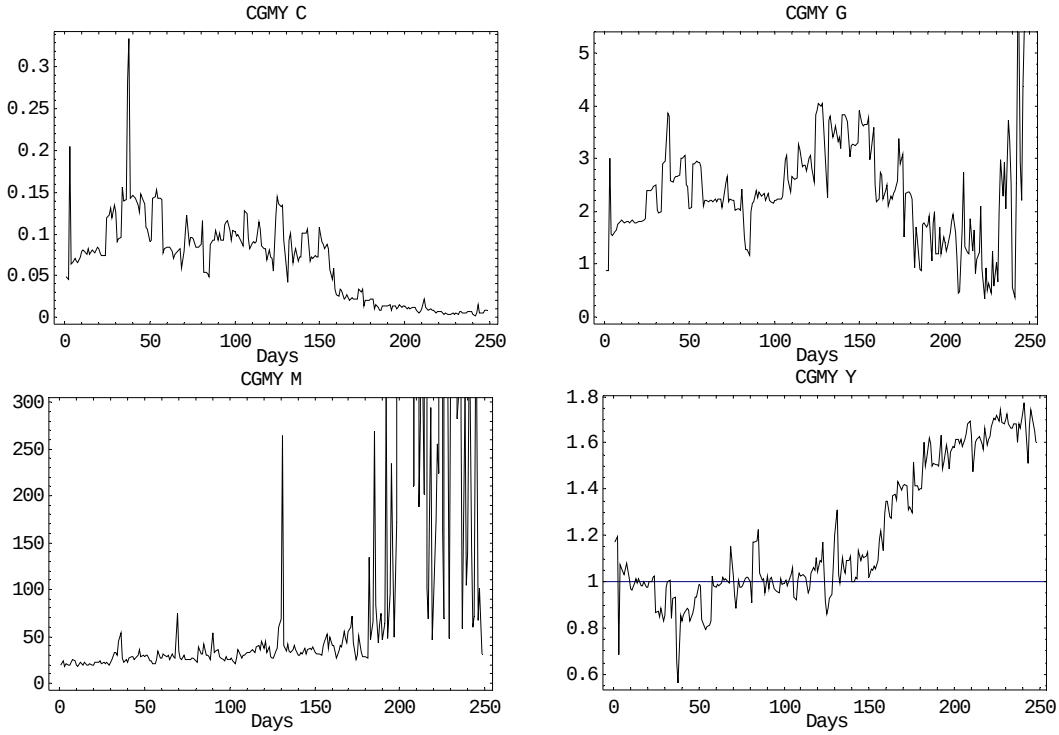

E) CGMY Model

Figure 5 Dynamics of Calibrated Parameters (Continued)

5.B Implied Dynamics of Log Return Probability Density Functions

Figure 6 reports the calibrated probability density functions of log returns on one day before last trading day March 16, 2005 as the time to maturity nears from 1 to 0 for each model.[z] For the purpose of clear illustration, Figure 7 reports the snapshots of Figure 6 on six different maturity dates and Figure 8 reports the time series of the implied moments of log return probability density function for each model. It is apparent that the extra parameters of various non-Gaussian Lévy models allow the negative skewness (i.e. fatter lower tail and thinner upper tail) and the excess kurtosis (i.e. higher peaked and heavier tailed) of the log return density over the BS model which is the only Gaussian

[z] Remember that the probability density function of the CGMY process is not available in closed form in the general case.

Lévy models. Notice from Figure 8 that all non-Gaussian Lévy models have the similar mean and variance, but the CGMY model has the higher negative skewness and the higher excess kurtosis especially for the short term to maturity.

Figure 9 reports the time series of the lower tail probabilities of implied log return probability density functions for each model. The lower tail probability is defined as the probability that the log return declines more than 10% on the day, i.e. $\mathbb{Q}(R_T < -0.1)$. We observe that the BS model overestimates the lower tail probability for the long term to maturity, but it underestimates that for the short term to maturity which is a very important factor for the risk management.

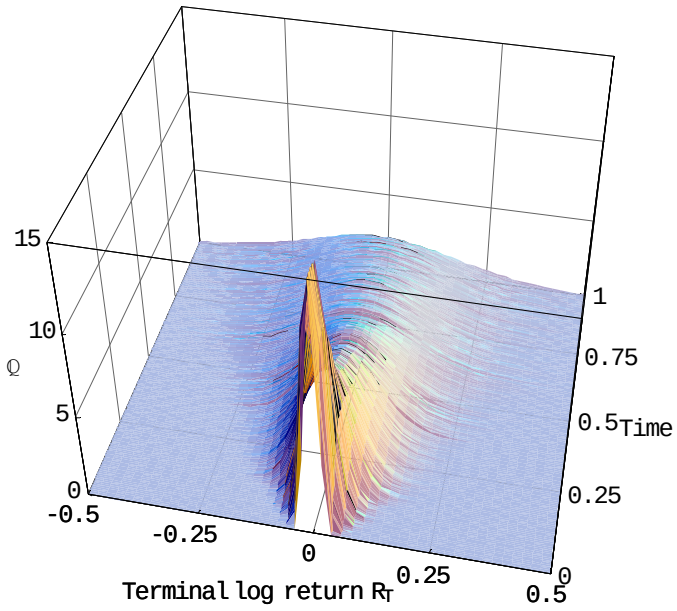

A) BS Model

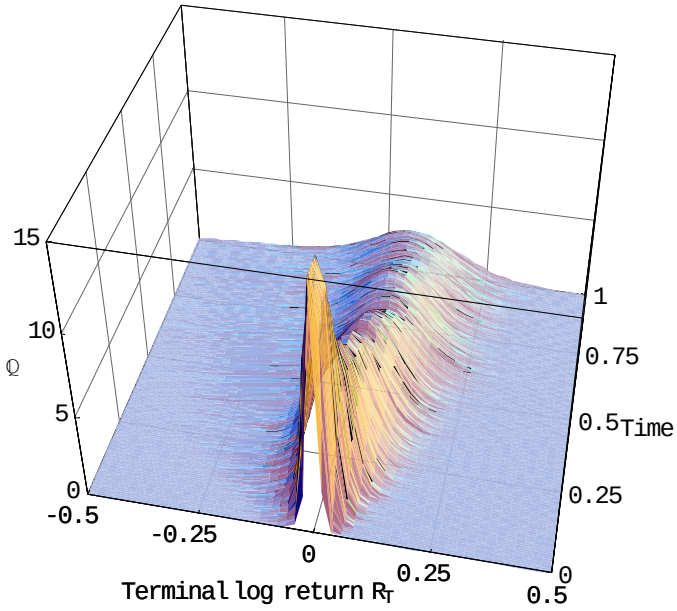

B) MJD Model

Figure 6 Implied Dynamics of Probability Density Functions of Log Returns
Calibrated probability density functions of log returns on one day before last trading day March 16, 2005 are plotted as the time to maturity nears from 1 to 0. Note that the above figures illustrate density functions only for the range of probability density between 0 and 15.

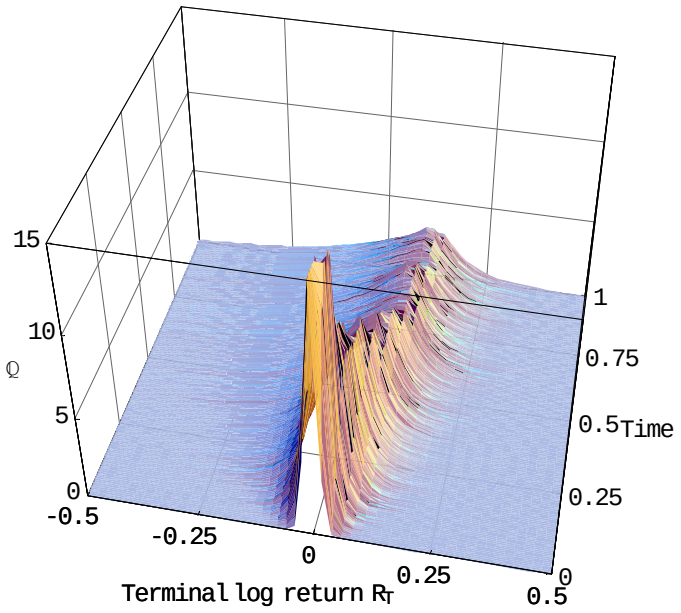

C) VG Model

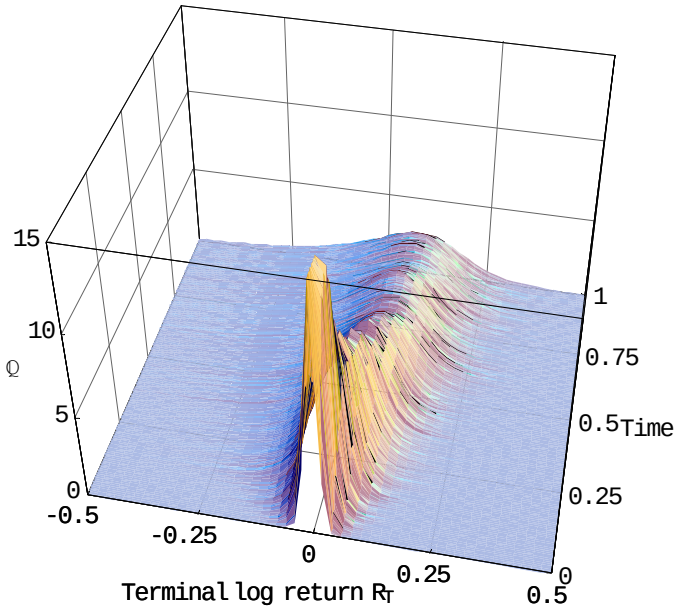

D) NIG Model

Figure 6 Implied Dynamics of Probability Density Functions of Log Returns (Continued)

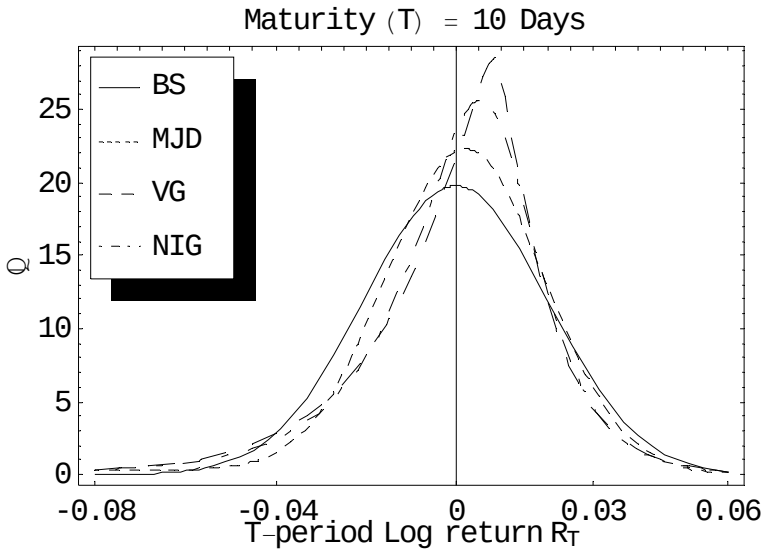

A) March 4, 2005. 10 days to maturity.

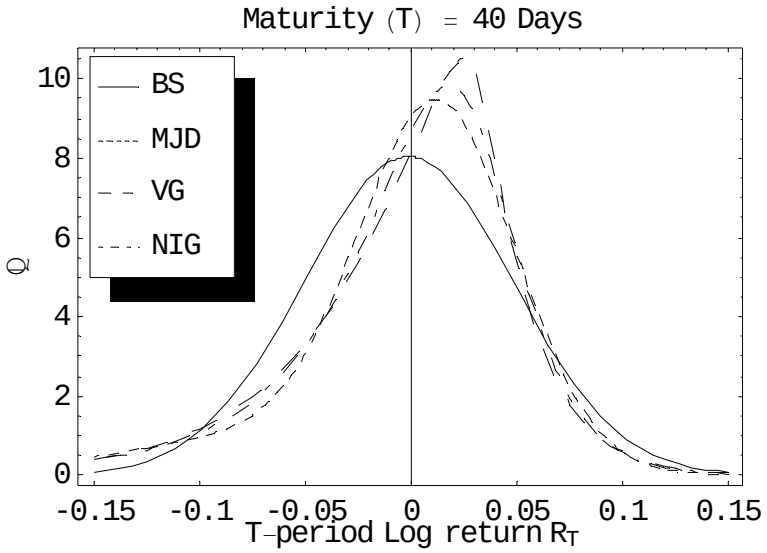

B) January 20, 2005. 40 days to maturity.

Figure 7 Plot of Implied Probability Density Functions of Log Returns On six different days, calibrated probability density functions of log returns on one day before last trading day March 16, 2005 are plotted.

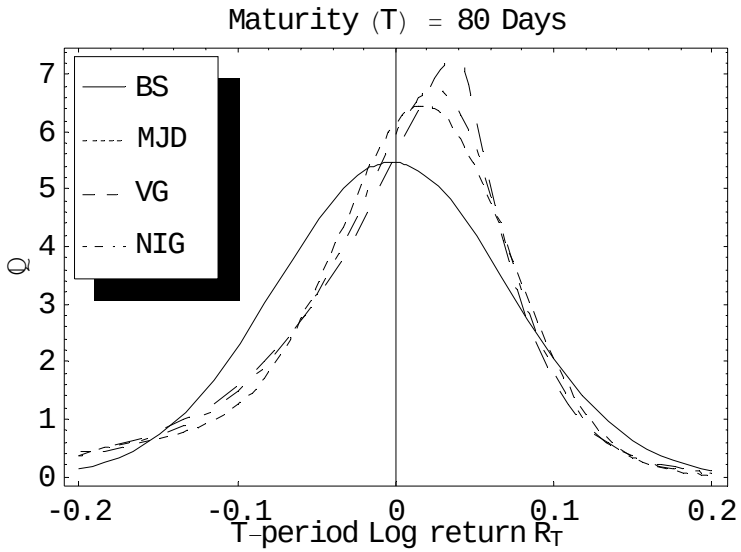

C) November 22, 2004. 80 days to maturity.

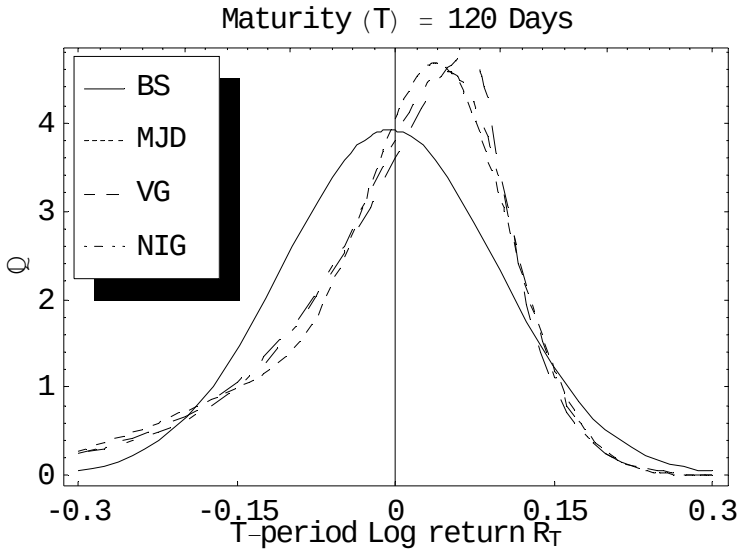

D) September 27, 2004. 120 days to maturity.

Figure 7 Plot of Implied Probability Density Functions of Log Returns (Continued)

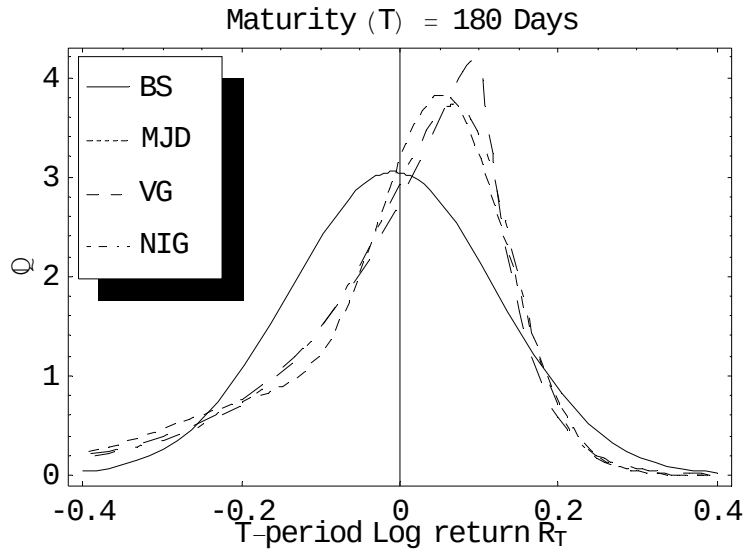

E) July 1, 2004. 180 days to maturity.

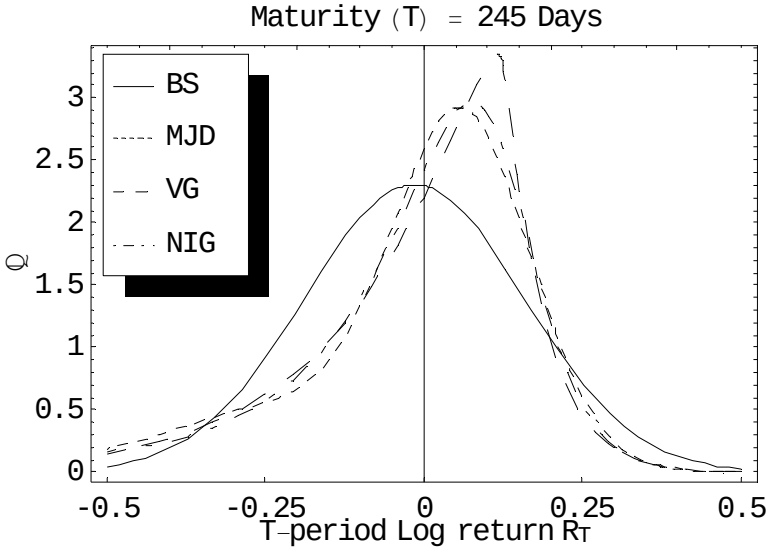

F) March 30, 2004. 245 days to maturity.

Figure 7 Plot of Implied Probability Density Functions of Log Returns (Continued)

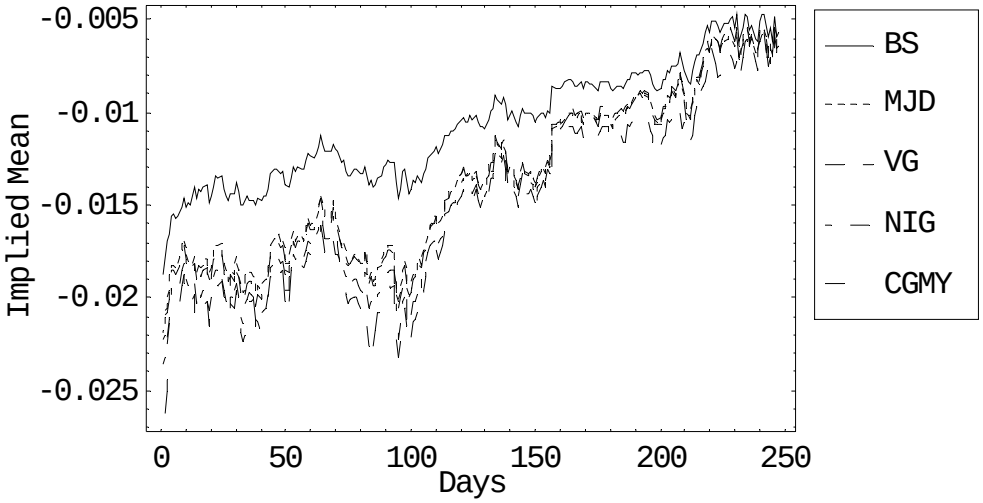

A) Implied Mean of Log Returns

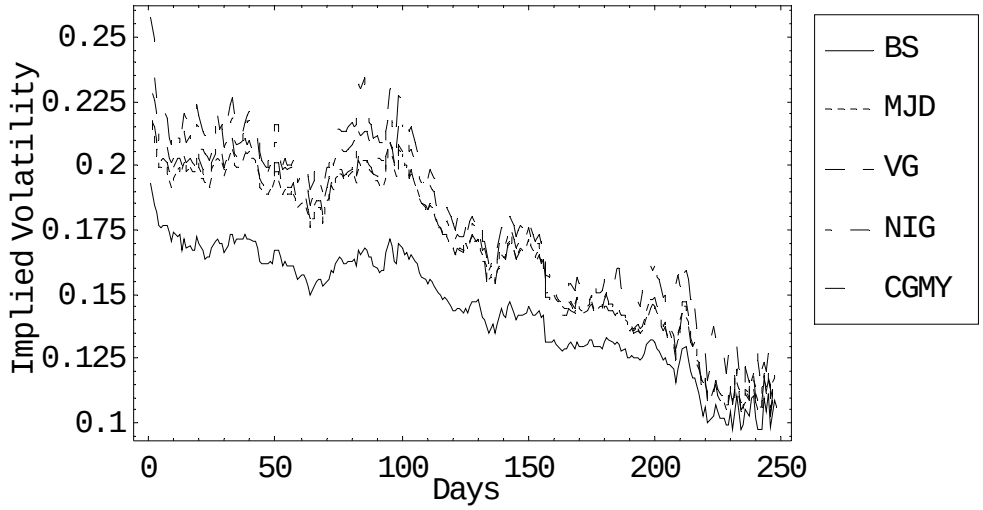

B) Implied Volatility of Log Returns

Figure 8 Dynamics of Implied Moments of Log Return Probability Density Functions Time series of implied moments of log return probability density functions on one day before last trading day March 16, 2005 are plotted for each model. Note that the day 1 is March 24, 2004 and the day 248 is March 16, 2005.

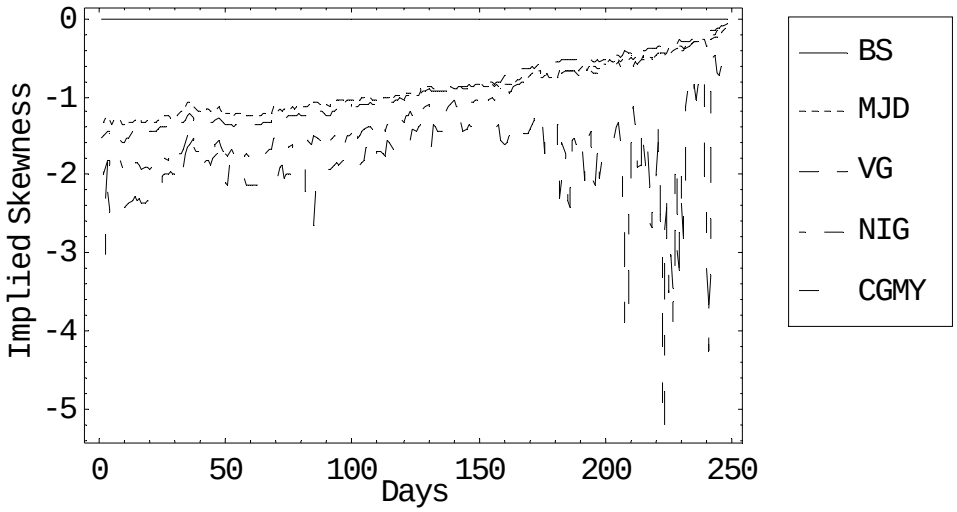

C) Implied Skewness of Log Returns

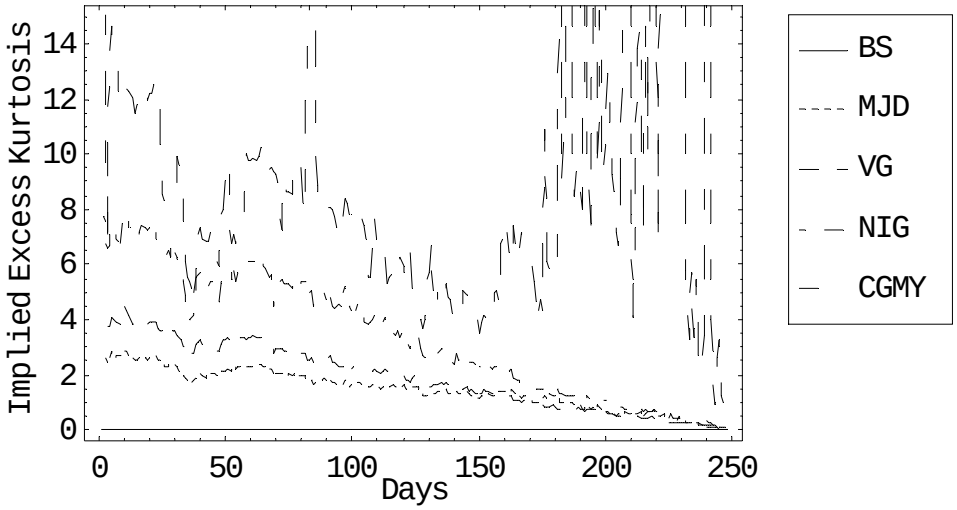

D) Implied Excess Kurtosis of Log Returns

Figure 8 Dynamics of Implied Moments of Log Return Probability Density Functions (Continued)

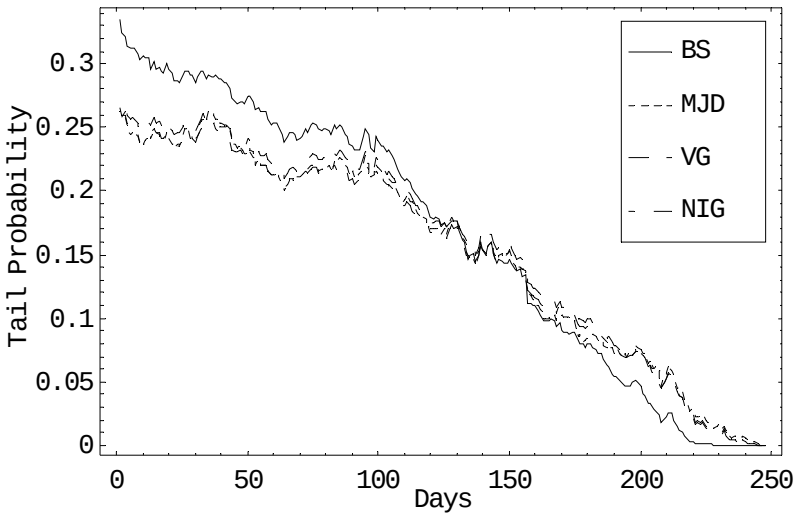

Figure 9 Dynamics of Lower Tail Probability of Implied Log Return Probability Density Functions Time series of the lower tail probabilities of implied log return probability density functions on one day before last trading day March 16, 2005 are plotted for each model. The lower tail probability is defined as the probability that the log return declines more than 10% on the day, i.e. $\mathbb{Q}(R_T < -0.1)$. Note that the day 1 is March 24, 2004 and the day 248 is March 16, 2005.

5.B Dynamics of Implied Lévy Density Functions of Log Returns

Figure 10 reports the calibrated Lévy density functions of log returns on one day before last trading day March 16, 2005 as the time to maturity nears from 1 to 0 for each model. For the purpose of clear illustration, Figure 11 reports the snapshots of Figure 10 on six different maturity dates.

As previously mentioned, we observe the pattern of increasing total mass of the MJD model's Lévy density which is equal to the parameter λ as the maturity nears since it tends to increase as illustrated by Panel B) of Figure 5. Also notice that the arrival rate of negative jumps is far larger than that of positive jumps.

In contrast to the MJD model's finite activity and symmetric Lévy density, all pure jump Lévy models are characterized by the asymmetric and infinite activity Lévy densities which all look similar except the CGMY model's Lévy density having much

thinner upper tail especially in the Panel B) of Figure 11 where the arrival rate of positive jumps are actually zero. As expected, all infinite activity Lévy densities have heavier lower tails indicating that the negative jumps are more likely to arrive than the positive jumps.

Figure 12 reports the time series of the implied lower tail Lévy measure of log returns of each model which is transformed into a table in Table 4 by dividing the entire sample into three subsamples depending on the maturity[aa]. We define the lower tail Lévy measure as the arrival rate of jumps of size greater than -10%, i.e. $\int_{-\infty}^{-0.1} \ell_X(x)dx$. We observe that the lower tail Lévy measures of all three pure jump Lévy models behave similarly and tend to decline as the maturity nears. This means that the arrival rate of large negative jumps declines as the maturity nears. But, interestingly, although the implied lower tail Lévy measure of MJD model tends to decreases as the maturity nears, it relatively stays higher than that of three pure jump Lévy models in the short term to maturity (0.2430 versus 0.1483, 0.1653, and 0.1470).

[aa] Read section 5.1.

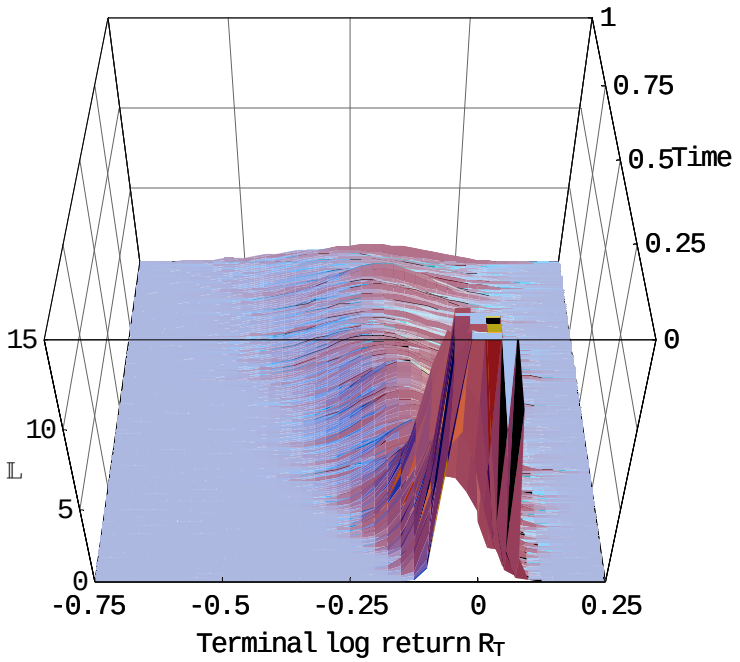

A) MJD Model

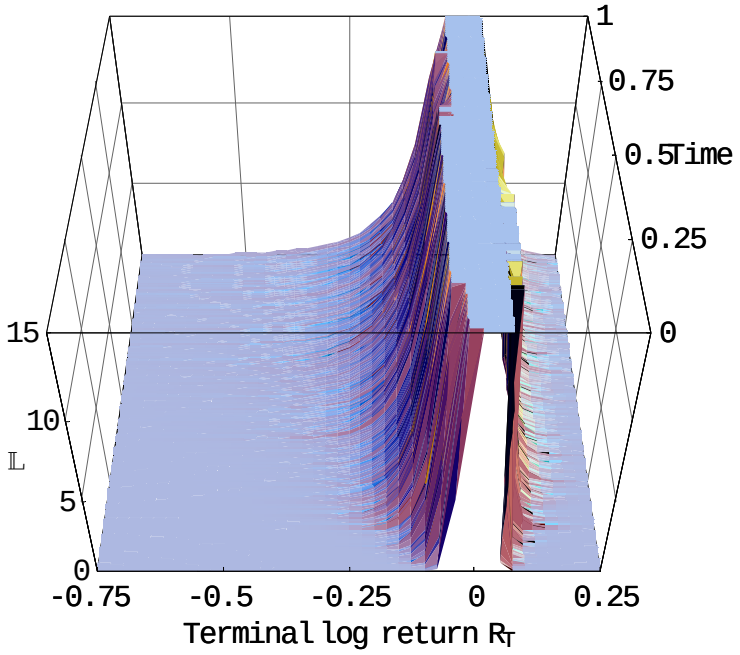

B) VG Model

Figure 10 Implied Dynamics of Lévy Density Functions of Log Returns Calibrated Lévy density functions of log returns on one day before last trading day March 16, 2005 are plotted as the time to maturity nears from 1 to 0. Note that the above figures illustrate the Lévy density functions only for the range of density between 0 and 15.

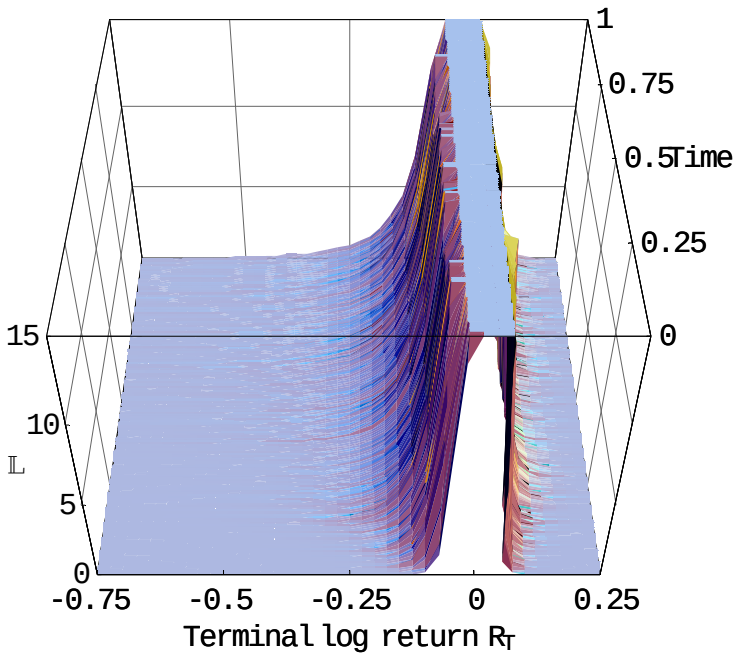

C) NIG Model

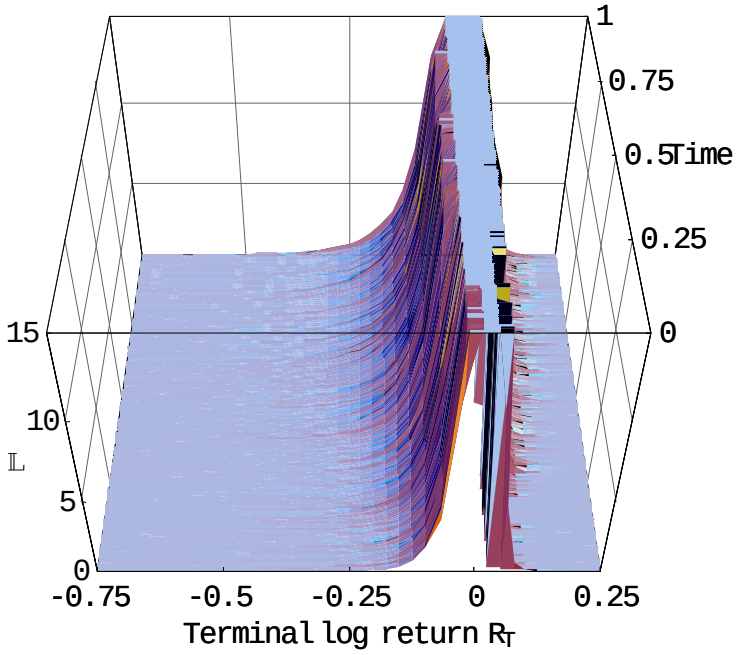

D) CGMY Model

Figure 10 Implied Dynamics of Lévy Density Functions of Log Returns (Continued)

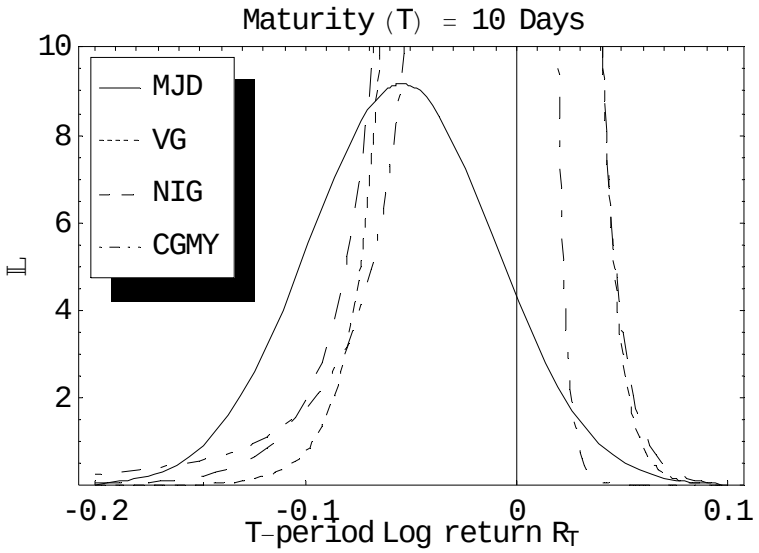

A) March 4, 2005. 10 days to maturity.

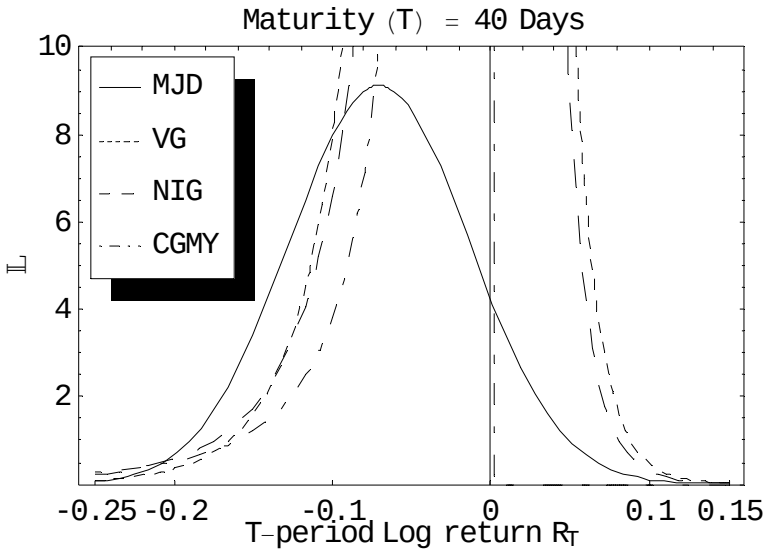

B) January 20, 2005. 40 days to maturity.

Figure 11 Plot of Implied Lévy Density Functions of Log Returns On six different days, calibrated Lévy density functions of log returns on one day before last trading day March 16, 2005 are plotted.

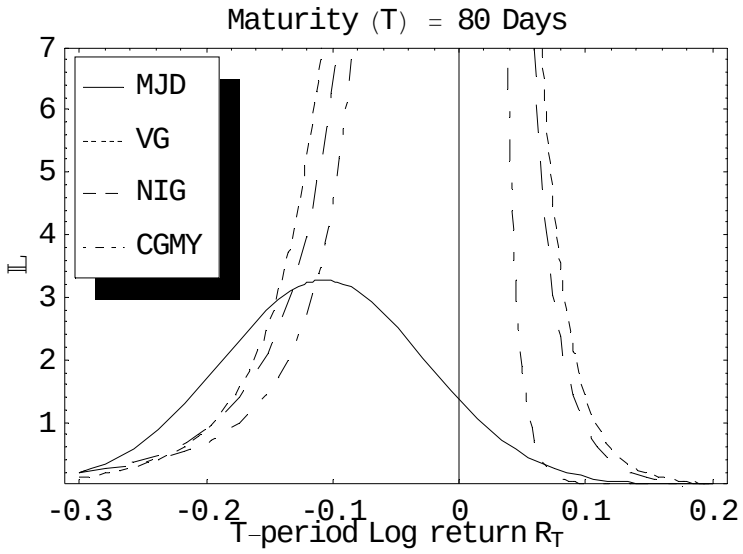

C) November 22, 2004. 80 days to maturity.

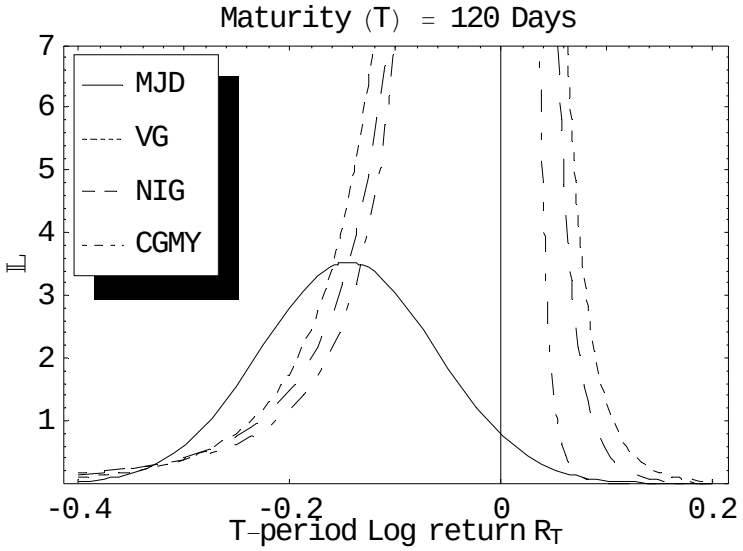

D) September 27, 2004. 120 days to maturity.

Figure 11 Plot of Implied Lévy Density Functions of Log Returns (Continued)

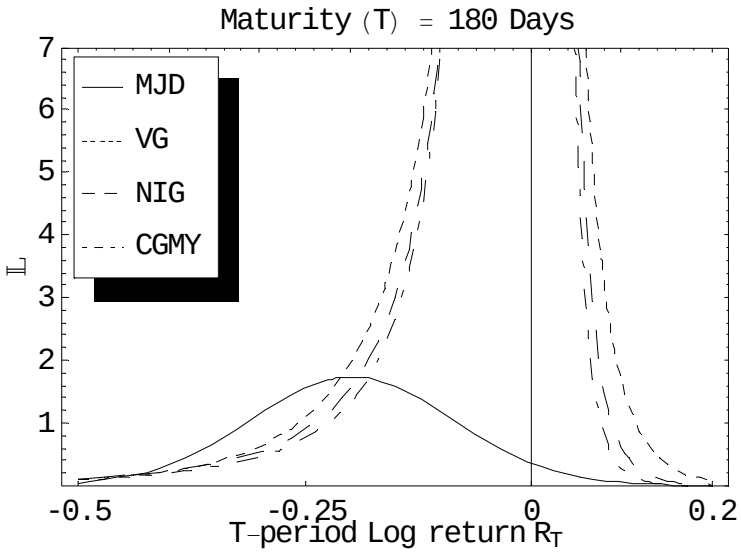

E) July 1, 2004. 180 days to maturity.

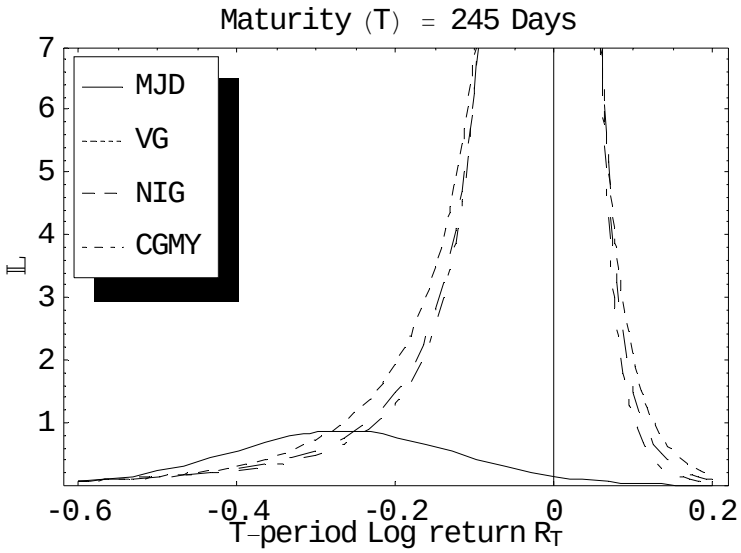

F) March 30, 2004. 245 days to maturity.

Figure 11 Plot of Implied Lévy Density Functions of Log Returns (Continued)

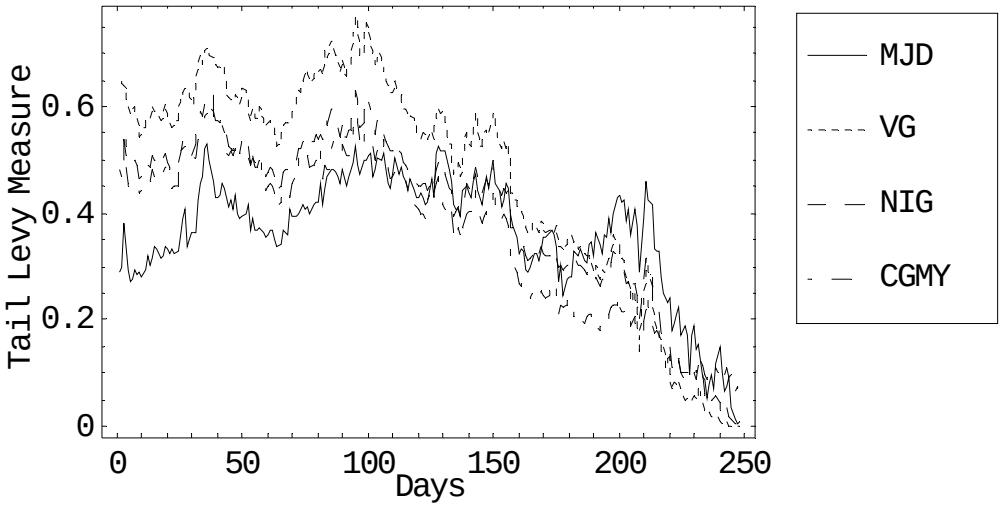

Figure 12 Implied Dynamics of Lower Tail Lévy Measure of Log Returns Time series of the implied lower tail Lévy measure of log returns on one day before last trading day March 16, 2005 are plotted for each model. The lower tail Lévy measure is defined as the arrival rate of jumps with the size greater than -10% on the day. Note that the day 1 is March 24, 2004 and the day 248 is March 16, 2005.

Table 4
Implied Dynamics of Lower Tail Lévy Measure of Log Returns
Time series of the implied lower tail Lévy measure of log returns in Figure 12 are made into a table for each model. The entire sample period is divided into three subperiods.

	Maturity (days)		
Model	long term (≥ 180)	medium term ($60 \leq \ < 180$)	short term (<60)
MJD	0.3695	0.4195	0.2430
VG	0.6077	0.5422	0.1483
NIG	0.5153	0.4532	0.1653
CGMY	0.4929	0.3978	0.1470

5.D In-Sample Performance of Lévy Models

In this section, in-sample fit of Lévy option pricing models is discussed although it bears little importance because in general more parameters lead to better in-sample fit. Table 5 reports the daily average, the standard error, the minimum, and the maximum of the sum of squared errors (SSE) for the sample period. Time series of the sum of squared errors on each day are plotted for each model by Figure 13. Figure 14 reports the in-

sample dollar pricing error defined as $C_i^{\text{model}}(S_0, K_i, T; \eta^{\mathbb{Q}}{}_0) - C_i^{\text{market}}$ across the varying moneyness and the time to maturity using a linear interpolation.

As expected, the BS model is by far the least fit model averaging the SSE of 327.314 because it has only one parameter σ. Panel A) of Figure 14 illustrates the well-known bias of the BS model which is to underprice the ITM (in-the-money, the moneyness K / F_0 less than one in the figure) calls and to overprice the OTM (out-of-the-money, the moneyness K / F_0 larger than one in the figure) calls. Or, through the put-call parity, the BS model underprices the OTM (the moneyness K / F_0 less than) puts and overprices the ITM (the moneyness K / F_0 larger than one in the figure) puts. This bias of the BS model becomes stronger especially for the short term OTM calls and puts in terms of the percentage mispricing errors because of the cheaper prices of the short term OTM calls and puts. Also, the volatility dynamics illustrated in Figure 15 can be used to explain the bias of the BS model since the BS model assumes the flat volatility surface, i.e. a constant volatility across the moneyness and the maturity. The observation that the volatility surface shifts from a declining smile to a V-shape as the maturity nears indicates the stronger bias of the BS model for the short term OTM calls and puts.

We see from Table 5 and Figure 13 that incorporating jumps in the underlying price process dramatically improves the in sample fit, but this is no surprise because of more parameters. The CGMY model has the best in-sample fit, the NIG model is the second, the MJD model is the third, and the VG model is the fourth. Panel B), C), D), and E) of

Figure 14 show no sign of systematic mispricing bias across the moneyness and the time to maturity of each of the jump Levy models.[bb]

Table 5
In-Sample Fit

The daily average, the standard error, the minimum, and the maximum of the sum of squared errors (SSE) for the sample period is presented.

Model	Daily Average	Standard Error	Minimum	Maximum
BS	327.314	170.428	0.77675	626.491
MJD	1.98586	2.42562	0.07417	10.1348
VG	4.38282	2.81334	0.13971	14.1986
NIG	1.62785	2.12555	0.06271	8.9489
CGMY	0.82602	1.24139	0.00435	5.5291

[bb] Note that the increasing underpricing for the short term OTM calls in the Panel B), C), D), and E) of Figure 14 is due to the linear extrapolation used and should be ignored. Short term deep OTM calls have prices of almost zero and go in the cabinet.

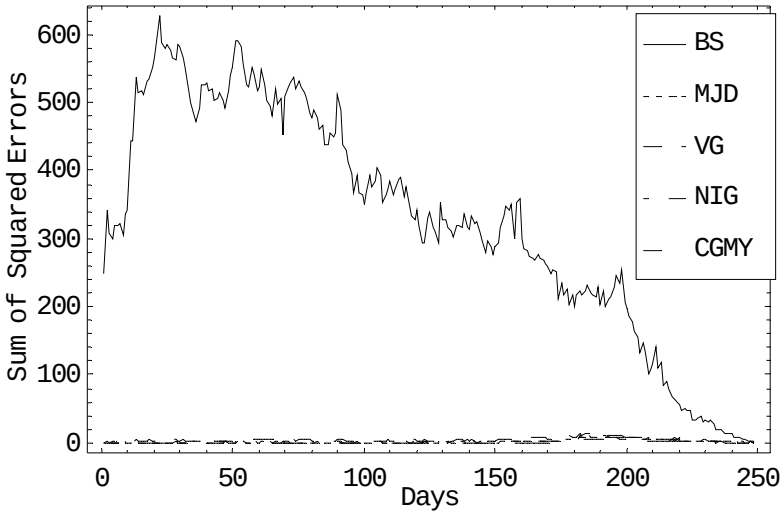

A) All Lévy Models.

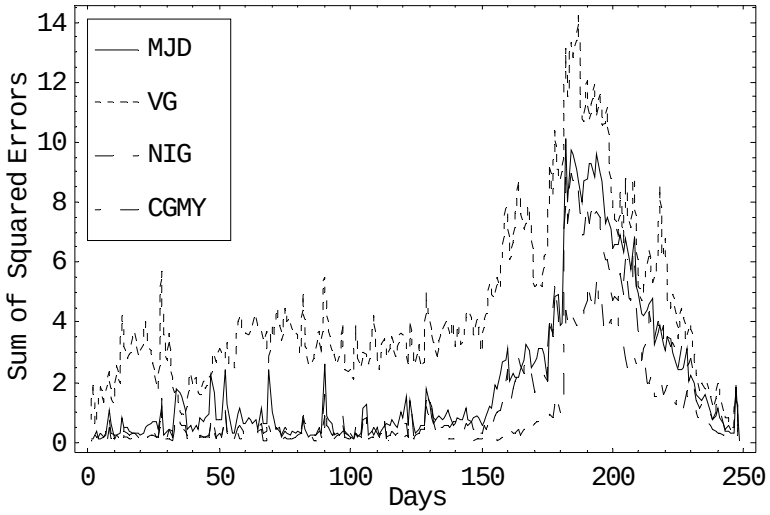

B) Jump Lévy Models.

Figure 13 Time Series Plot of Sum of Squared Errors Time series of the sum of squared errors on each day are plotted for each model. Note that the day 1 is March 24, 2004 and the day 248 is March 16, 2005.

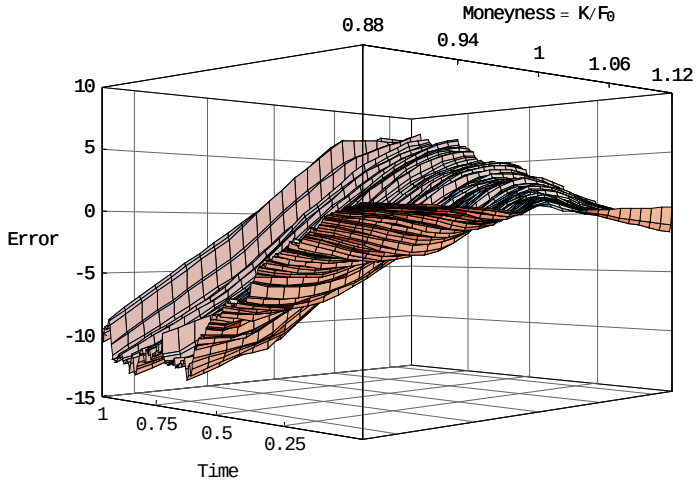

A) BS Model

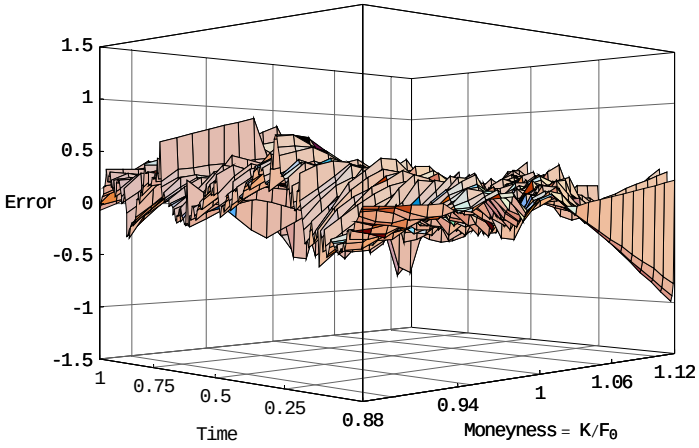

B) MJD Model

Figure 14 Dynamics of In-Sample Dollar Pricing Errors In-sample dollar pricing error defined as $C_i^{\text{model}}(S_0, K_i, T; \eta^{\mathbb{Q}}{}_0) - C_i^{\text{market}}$ is calculated on each day and plotted in a 3D figure across the varying moneyness and the time to maturity using a linear interpolation. Note that the time to maturity is measured in years.

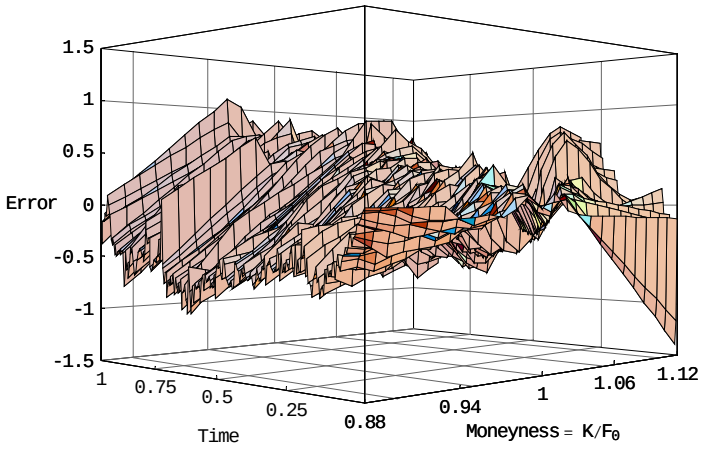

C) VG Model

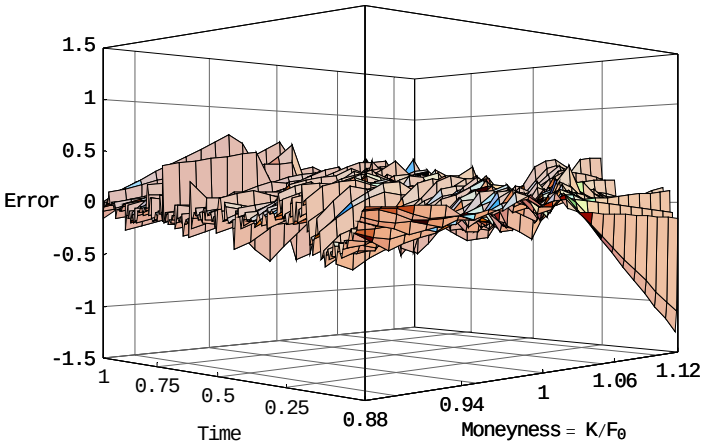

D) NIG Model

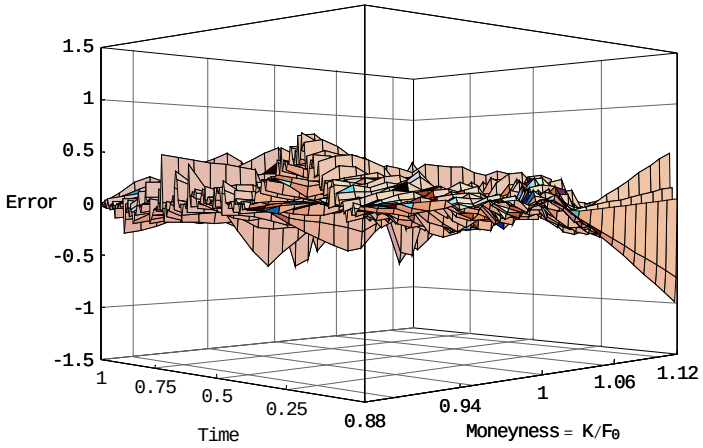

E) CGMY Model

Figure 14 Dynamics of In-Sample Dollar Pricing Errors (Continued)

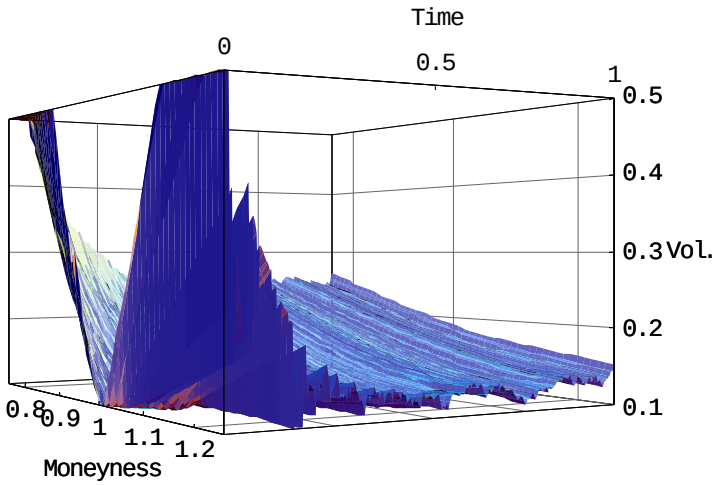

Figure 15 Volatility Dynamics BS implied volatilities are backed out across varying moneyness on each day and they are linearly interpolated. Note that the time to maturity is measured in years.

6. Out-of-Sample Pricing Performance of Lévy Models

We saw in the previous section that incorporating jumps in the underlying price process dramatically improves the in sample fit with the CGMY model being the best, the NIG model being the second, the MJD model being the third, and the VG model being the fourth. In this section, the more important out-of-sample fit of the each Lévy model is examined following Bakshi, Cao, and Chen (1997) because of the fact that the better in-sample fit might be due to more parameters of the jump Lévy models than the BS model. In other words, if the extra parameters of the jump Lévy models are redundant, they overfit the data and may produce larger out-of-sample fitting errors.

The procedure is as follows. Let t denote today. Firstly, on yesterday ($t-1$), the parameters of each Lévy model are recovered using the yesterday's call prices and variables. Secondly, today's model prices are computed using the yesterday's calibrated parameters ${\eta^{\mathbb{Q}}}_{t-1}$ and today's variables. Thirdly, using today's model prices and today's call prices, the absolute pricing error is obtained following the equation (61):

$$\text{absolute pricing error} = \left| C_t^{\text{model}}(F_t, K, T-t; {\eta^{\mathbb{Q}}}_{t-1}) - C_t^{\text{market}} \right|. \tag{61}$$

We repeat this procedure everyday across all the call strike prices. Figure 16 reports the time series of the daily sample average of absolute pricing error (i.e. the absolute pricing error per call option) for each Lévy models. As expected, the jump Lévy models overwhelmingly outperforms the BS model. But it is difficult to distinguish the out-of-sample fitting performance of each jump Lévy model. For this reason, Table 6 reports the out-of-sample absolute pricing errors per call option for total of 15 different subsamples. Note that the entire sample is divided according to its maturity and its moneyness. The long term is defined as more than or equal to 180 days to maturity and the short term is

less than 60 days to maturity. We define the deep ITM as the moneyness less than 0.94, the moneyness between 0.94 and 0.98 is ITM, the moneyness between 0.98 and 1.02 is ATM, the moneyness between 1.02 and 1.06 is OTM, and the moneyness greater than 1.06 is deep OTM. Note that we define the moneyness as K / F_0 which is an opposite of the definition of the moneyness used by Bakshi, Cao, and Chen (1997).

We firstly observe from Table 6 that in terms of the absolute pricing error per call, the CGMY model is the best with having the least error in 11 subsamples out of 15, the NIG model is the second with having the least error in 4 subsamples and having the second least error in 5 subsamples, the MJD model is the third with having the least error in 1 subsamples and having the second least error in 7 subsamples, and the VG model is the fourth although it is a significant improvement over the BS model. For example, for the out-of-sample pricing of the medium term ATM calls, the CGMY model has the least absolute dollar pricing error per call with \$0.598, the MJD model is the second best with \$0.602, the NIG model is the third with \$0.612, the VG model is the fourth with \$0.685, and the BS model has the largest error of \$1.365. It is interesting to find that the MJD model which is a finite activity Lévy model containing a Brownian motion outperforms the VG model which is an infinite activity Lévy model of finite variation with pure jump sample paths. This indicates that the MJD model is still usable for the purpose of index option pricing. One extremely important observation is that the CGMY model is outperformed by the other jump Lévy models for the short term deep OTM calls. For the short term deep OTM calls, the NIG model performs the best with the absolute error per call \$0.12, the MJD model is the second with \$0.14, the VG model is the third with \$0.165, and the CGMY model is the fourth with \$0.188. Thus, the pricing excellence of

the CGMY model for overall option pricing should be interpreted with a caution. Also note that the absolute pricing error of each model tends to decrease as the maturity nears for each moneyness as pointed out by Bakshi, Cao, and Chen (1997).

In order to closer examine the out-of-sample pricing bias associated with the Lévy models, out-of-sample dollar pricing error (not the absolute value, therefore it can show underpricing or overpricing) defined as $C_t^{\text{model}}(F_t, K, T-t; \eta^{\mathbb{Q}}_{t-1}) - C_t^{\text{market}}$ is calculated on each day across different strike prices and plotted in a 3D figure across the varying moneyness and the time to maturity using a linear interpolation. As expected and previously mentioned, we observe the bias of the BS model which is to underprice the ITM calls and to overprice the OTM calls. Interestingly, the dynamics of out-of-sample dollar pricing error of all jump Lévy models resemble one another which differ significantly from the BS counterpart. We find that jump Lévy models either underprices or overprices all calls on a given day and the size of the dollar pricing error is largest near ATM calls because of the bell-shaped or reverse bell-shaped pattern. Thus, the jump Lévy models still possess the pricing bias associated with the moneyness and the maturity although it is much smaller than the BS model.

Out-of-sample pricing performance of each Lévy model can also be evaluated by the orthogonality test which is based on the idea that a good model should not possess any consistent pattern in pricing errors and the pricing errors of a good model cannot be predicted. Our orthogonality test is conducted by regressing the out-of-sample dollar pricing errors ε_i on the moneyness K_i / F_0, the moneyness squared $(K_i / F_0)^2$, the time to maturity T_i, and the interest rate r_i:

$$\varepsilon_i = \beta_0 + \beta_1 (K_i / F_0) + \beta_2 (K_i / F_0)^2 + \beta_3 T_i + \beta_4 r_i + e_i . \tag{62}$$

Note that Carr, Chang, and Madan (1998) employ this type of orthogonality test for the in-sample pricing performance of the VG model, ours is for the out-of-sample pricing performance. The results of the orthogonality test are shown in Table 7. We firstly notice that the orthogonality of the out-of-sample pricing errors for all Lévy models are rejected because of the high values for the $F-$statistic which are in row 8. This means that the out-of-sample pricing errors for all Lévy models can be explained by the moneyness, the moneyness squared, the time to maturity, and the interest rate which all have coefficients significantly different from zero shown in row 1 through row 5. These biases of all Lévy models can be intuitively seen from Figure 17. But, in terms of the degree of bias, the BS model is the most biased. In other words, the pricing errors of the BS model are the most predictable with the adjusted R^2 of 47%. The least biased model is the CGMY with the adjusted R^2 of 2.4%. The MJD and the NIG models are the second best with the adjusted R^2 of 6.9% which outperform the VG model with the adjusted R^2 of 11.1%.

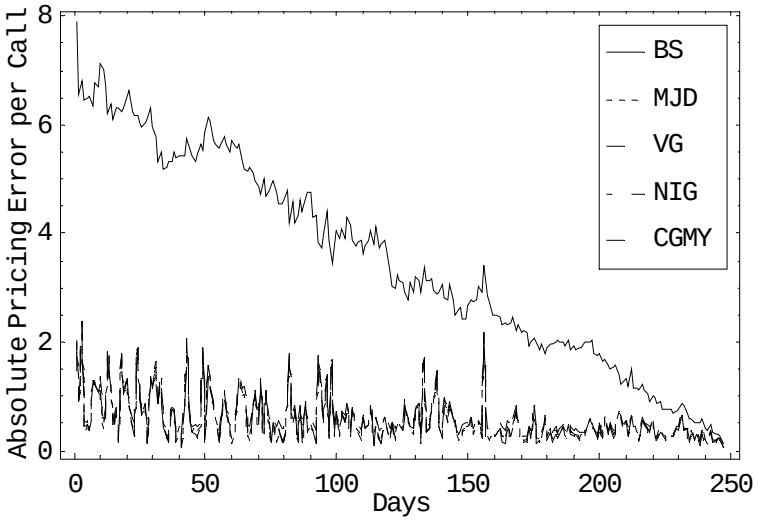

A) All Lévy Models.

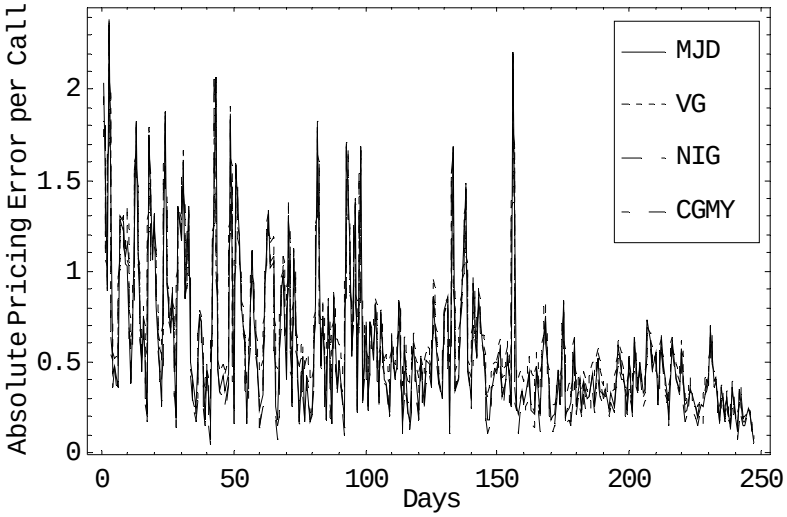

B) Jump Lévy Models.

Figure 16 Time Series Plot of Absolute Pricing Errors per Call Option Time series of the absolute pricing error per call are plotted for each Lévy models. Note that the day 1 is March 24, 2004 and the day 248 is March 16, 2005.

Table 6
Out-of-Sample Absolute Pricing Errors per Call Option

Today's model price is computed using the yesterday's implied parameters for each call option. We define the absolute pricing error per option as the sample average of the absolute difference between the market price and the model price. Note that the entire sample is divided according to its maturity and its moneyness. The long term is defined as more than or equal to 180 days to maturity and the short term is less than 60 days to maturity. We define the deep ITM as the moneyness less than 0.94, the moneyness between 0.94 and 0.98 is ITM, the moneyness between 0.98 and 1.02 is ATM, the moneyness between 1.02 and 1.06 is OTM, and the moneyness greater than 1.06 is deep OTM.

		Moneyness K / F_0				
Days to Expiration	Model	< 0.94	0.94 – 0.98	0.98 – 1.02	1.02 – 1.06	> 1.06
≥ 180	BS	$11.14	$5.568	$2.493	$2.527	$5.861
	MJD	0.802	1.016	1.056	0.958	0.626
	VG	0.881	1.065	1.173	1.006	0.696
	NIG	0.788	0.965	1.064	0.967	0.609
	CGMY	0.799	0.938	1.047	0.966	0.609
60 – 180	BS	5.278	3.598	1.365	2.047	2.774
	MJD	0.575	0.514	0.602	0.586	0.347
	VG	0.694	0.613	0.685	0.649	0.436
	NIG	0.504	0.537	0.612	0.589	0.348
	CGMY	0.420	0.477	0.598	0.579	0.337
< 60	BS	1.258	1.703	0.794	1.264	0.615
	MJD	0.417	0.399	0.507	0.282	0.140
	VG	0.493	0.386	0.516	0.300	0.165
	NIG	0.400	0.379	0.506	0.271	0.120
	CGMY	0.265	0.374	0.503	0.284	0.188

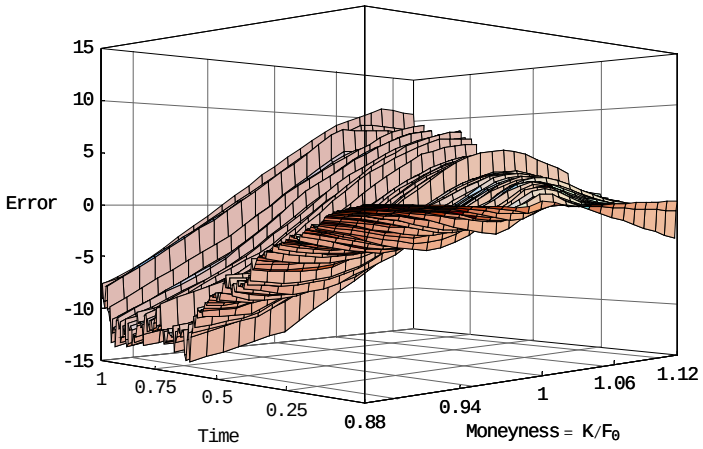

A) BS Model

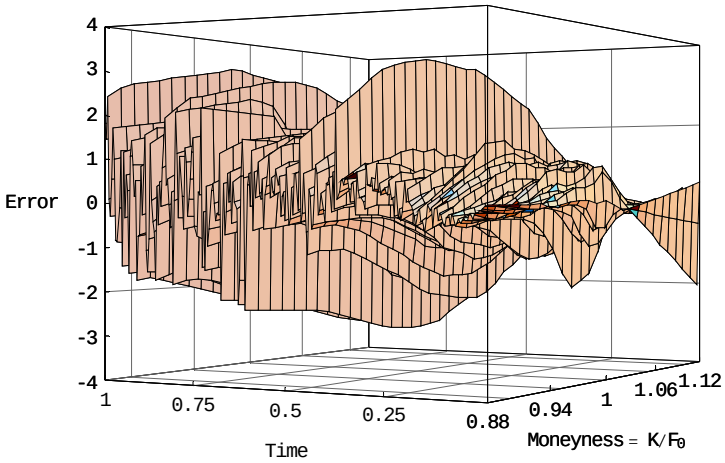

B) MJD Model

Figure 17 Dynamics of Out-of-Sample Dollar Pricing Errors Out-of-sample dollar pricing error defined as $C_t^{\text{model}}(F_t, K, T-t; \eta^{\mathbb{Q}}_{t-1}) - C_t^{\text{market}}$ is calculated on each day across different strike prices and plotted in a 3D figure across the varying moneyness and the time to maturity using a linear interpolation. Note that the time to maturity is measured in years.

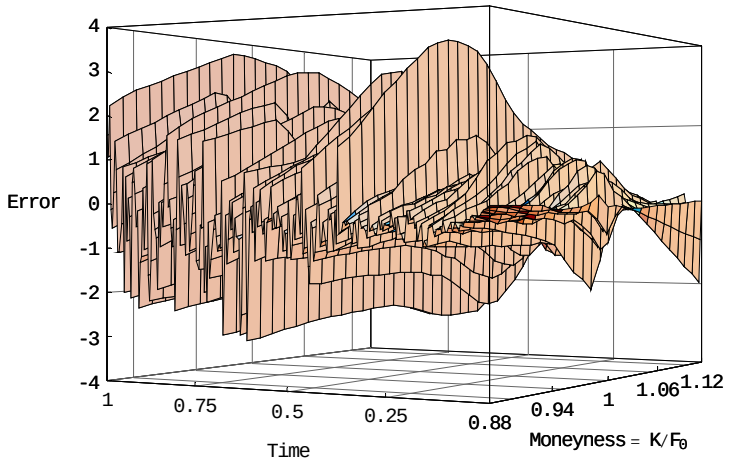

C) VG Model

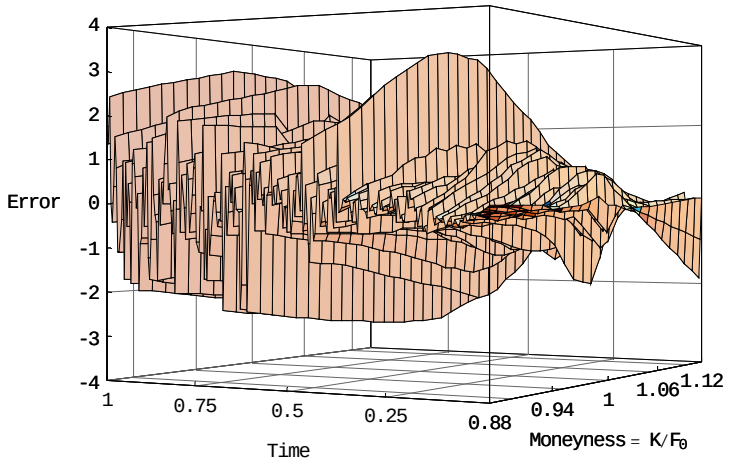

D) NIG Model

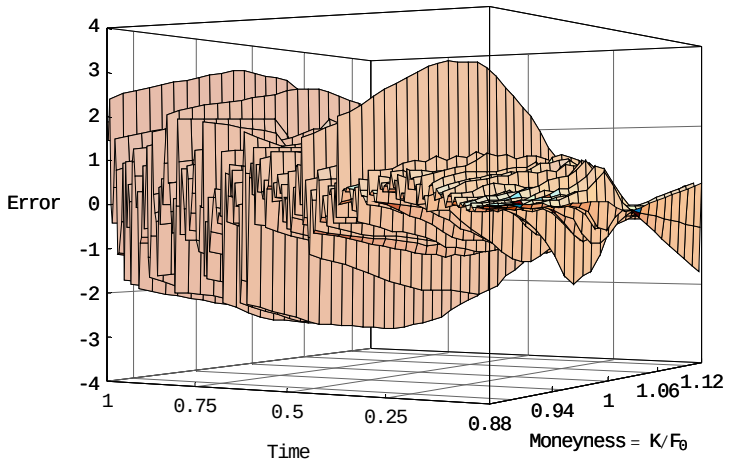

E) CGMY Model

Figure 17 Dynamics of Out-of-Sample Dollar Pricing Errors (Continued)

Table 7
Orthogonality Test Results of Out-of-Sample Dollar Pricing Errors

Out-of-sample dollar pricing errors ε_i are regressed on the moneyness K_i / F_0, the moneyness squared $(K_i / F_0)^2$, the time to maturity T_i, and the interest rate r_i:

$$\varepsilon_i = \beta_0 + \beta_1 (K_i / F_0) + \beta_2 (K_i / F_0)^2 + \beta_3 T_i + \beta_4 r_i + e_i .$$

t-statistics are in parentheses. * indicates the significance at 5% level.

Independent variable	BS	MJD	VG	NIG	CGMY
β_0	-15.227	-10.864	-11.726	-10.353	-6.602
(1)	(-6.744)*	(-18.929)*	(-19.050)*	(-18.262)*	(-11.819)*
β_1	-21.898	17.529	17.700	16.672	10.959
(K_i / F_0)	(-5.852)*	(18.427)*	(17.345)*	(17.744)*	(11.837)*
β_2	23.439	-8.351	-7.879	-7.863	-5.496
$((K_i / F_0)^2)$	(12.481)*	(-17.492)*	(-15.388)*	(-16.673)*	(-11.827)*
β_3	7.415	1.436	1.481	1.295	1.022
(T_i)	(7.445)*	(5.671)*	(5.453)*	(5.176)*	(4.147)*
β_4	522.964	63.646	72.040	58.544	43.140
(r_i)	(10.462)*	(5.009)*	(5.286)*	(4.664)*	(3.488)*
Adjusted R^2	0.472	0.069	0.111	0.069	0.024
Observations	6567	6567	6567	6567	6567
F statistic$_{(4, 6567)}$	1464.14	122.477	204.886	122.179	41.776

7. Conclusion

We calibrated a total of five different Lévy models to the S&P 500 futures options. The classic Black-Scholes model is the only continuous (i.e. Gaussian) Lévy model in which the asset price dynamics is modeled by the Brownian motion. Another classic Merton jump diffusion model is the non-Gaussian Lévy model in which the asset price dynamics is modeled by the jump diffusion process which possesses the discontinuities although they are rare. And, relatively recently developed three pure jump Lévy models in which the asset price dynamics is modeled using pure jump Lévy process. They are the variance gamma model, the normal inverse Gaussian model, and the CGMY model. Carr and Madan's (1999) Fourier transform option pricing approach with the modified call price was employed for the pricing.

The calibration result suggests that the extra parameters of various jump Lévy models allow the negative skewness and the excess kurtosis of the log return density over the BS model. On the dynamics of implied Lévy density functions of log returns, we observe the pattern of increasing total mass of the MJD model's symmetric Lévy density. And, the Lévy densities of all pure jump Lévy models are characterized by the asymmetric and infinite activity Lévy densities which all resemble one another. In terms of the out-of-sample pricing performance, containing jumps in the underlying price process drastically improves the performance over the BS model. As expected, the BS model is the least fit and it possesses the strong bias of underpricing the ITM calls and overpricing the OTM calls. Which jump Lévy models perform the best in pricing? The answer should be interpreted with a caution. The CGMY model is the least biased model in terms of overall pricing meaning that its pricing errors are the most unpredictable. But

other jump Lévy models (MJD, VG, and NIG) outperform the CGMY model for the short term deep OTM calls. Another result is that the classic MJD model which contains a Brownian motion performs as good as the NIG model and consistently outperforms the VG models for the pricing of index options. As Bakshi, Cao, and Chen (1998) point out that all option pricing models are misspecified (biased) because the correctly specified (unbiased) model would produce errors which are on average equal to zero. In our context, all the Lévy models are misspecified with regard to the moneyness and the maturity, most notably. But, we find that adding jumps in the underlying price process drastically reduces the degree of misspecification of the model.

We would like to suggest a couple of topics for the future research. One is that this paper can be reapplied to the other data such as individual stock options, commodity options (such as oil), and the currency options. It is very likely that the empirical result changes. More interesting and challenging topic would be the hedging with jump Lévy models. Because jumps are non-traded source of risk, jump Lévy models are incomplete models which do not allow for arbitrage pricing. We intend to deal this topic in the near future.

Appendix

A.1 Gamma Process

A gamma process $(Z_{t\in[0,\infty)})$ defined on a filtered probability space $(\Omega, \mathcal{F}_{t\in[0,\infty)}, \mathbb{P})$ with the Lévy triplet $(A_Z = 0, \ell_Z, \gamma_Z = 0)$ is a real valued stochastic process whose increments are distributed as the gamma distribution:

(A.1) $$\mathbb{P}_G(z_t; \mu_G, \nu) = \left(\frac{\mu_G}{\nu}\right)^{\frac{\mu_G{}^2}{\nu}t} \frac{z^{\frac{\mu_G{}^2}{\nu}t-1} \exp\left(-\frac{\mu_G}{\nu}z\right)}{\Gamma\left(\frac{\mu_G{}^2}{\nu}t\right)} 1_{z>0},$$

where $\mu_G \in \mathbb{R}^+$ is called a mean rate and $\nu \in \mathbb{R}^+$ is called a variance rate of the gamma process because the mean and variance of the gamma process are given by:

(A.2) $$E[Z_t] = \mu_G t,$$

$$Variance[Z_t] = \nu t.$$

Setting $\mu_G = 1$ produces the gamma process with unit mean rate whose increments are distributed as the gamma distribution with one parameter $\mathbb{P}_G(z_t; \nu)$ of the equation (2.1).

The gamma process with the Lévy triplet $(A_Z = 0, \ell_Z, \gamma_Z = 0)$ is a special case of a real valued non-degenerate tempered strictly stable subordinator (i.e. increasing Lévy process) when its stability index satisfies $\alpha_S = 0$. Consult Cont and Tankov (2004) for details. Gamma subordinator is a pure jump Lévy process because its Gaussian variance

is zero $A_Z = 0$ (Lévy-Itô decomposition). Since the gamma process is a subordinator, its Lévy measure $\ell_Z(z)$ is concentrated on the positive half axis (i.e. no negative jumps):

$$\int_{-\infty}^{0} \ell_Z(z)dz = 0 .$$

The Lévy measure of the gamma subordinator with unit mean rate is given by:

$$\ell_Z(z;\nu) = \frac{1}{\nu}\frac{\exp(-z/\nu)}{z}1_{z>0} .$$

The gamma subordinator is an infinite activity Lévy process because the total mass of the Lévy measure is infinite:

$$\int_{0}^{\infty} \ell_Z(z)dz = \infty .$$

The gamma subordinator is a Lévy process of finite variation because it satisfies:

$$\int_{|z|<1} |z|\,\ell_Z(z)dz < \infty ,$$

which can be further simplified as follows since subordinators have only positive jumps:

$$\int_{(0,1)} z\ell_Z(z)dz < \infty .$$

Consult theorem 3.11 of Matsuda (2005a).

A.2 Inverse Gaussian Process

The inverse Gaussian process $(Z_{t\in[0,\infty)})$ defined on a filtered probability space $(\Omega, \mathcal{F}_{t\in[0,\infty)}, \mathbb{P})$ with the Lévy triplet $(A_Z = 0, \ell_Z, \gamma_Z = 0)$ is a real valued stochastic process whose increments are distributed as the IG distribution:

$$\text{(A.3)} \qquad \mathbb{P}_{IG}(z_t;\delta,\gamma) = \frac{\delta t}{\sqrt{2\pi}} z_t^{-3/2} \exp\left(\delta\gamma t\right) \exp\left\{-\frac{\left(\gamma^2 z_t + \delta^2 t^2 z_t^{-1}\right)}{2}\right\} 1_{z>0},$$

where $\delta \in \mathbb{R}^+$ and $\gamma \in \mathbb{R}^+$. The standardized moments of the IG process are obtained as:

(A.4)
$$E[Z_t] = \frac{\delta t}{\gamma},$$

$$Variance[Z_t] = \frac{\delta t}{\gamma^3},$$

$$Skewness[Z_t] = \frac{3}{\sqrt{\delta t \gamma}},$$

$$Excess\ Kurtosis[Z_t] = \frac{15}{\delta t \gamma}.$$

Note that the standardized moments (A.4) tell us that the IG probability density is always positively skewed and the excess kurtosis is always positive. Figure A.2.1 illustrates the shape of the IG distribution with varying parameters. In Panel A, as γ increases holding δ constant, all the standardized moments decrease. In Panel B, as δ rises holding γ constant, the mean and variance rise while the skewness and excess kurtosis fall.

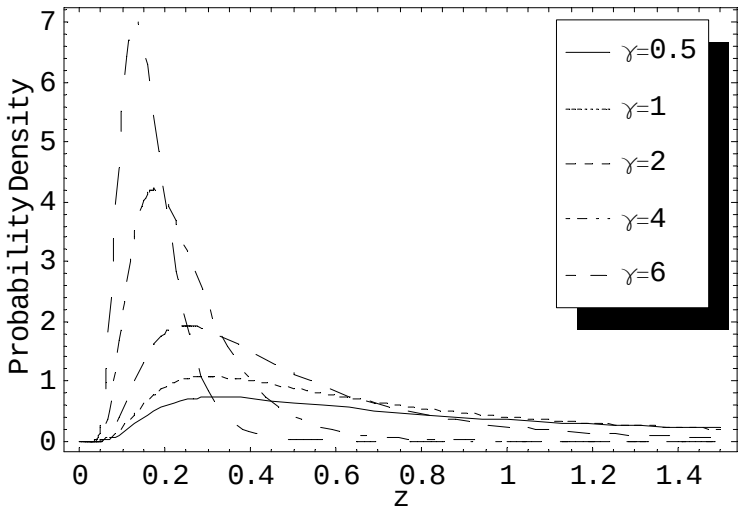

A) δ = 1 and varying γ

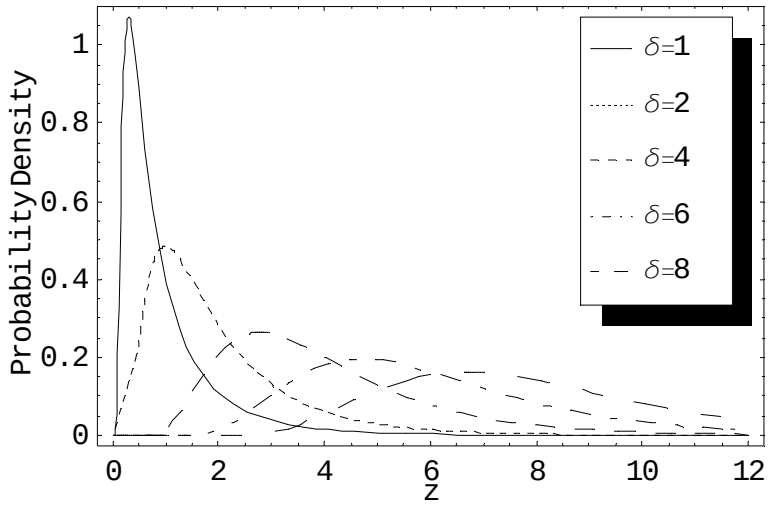

B) Varying δ and γ = 1

Figure A.2.1. Plot of IG probability density

The IG process with the Lévy triplet $(A_Z = 0, \ell_Z, \gamma_Z = 0)$ is a special case of a real valued non-degenerate tempered strictly stable subordinator (i.e. increasing Lévy process) when its stability index satisfies $\alpha_S = 1/2$. Consult Cont and Tankov (2004) for details. IG subordinator is a pure jump Lévy process because its Gaussian variance is zero $A_Z = 0$ (Lévy-Itô decomposition). Since the IG process is a subordinator, its Lévy measure $\ell_Z(z)$ is concentrated on the positive half axis (i.e. no negative jumps):

$$\int_{-\infty}^{0} \ell_Z(z)dz = 0 .$$

The Lévy measure of the IG subordinator is given by:

$$\ell_Z(z;\delta,\gamma) = \frac{\delta}{\sqrt{2\pi}} \frac{\exp\left(-\frac{\gamma^2}{2} z\right)}{z^{3/2}} 1_{z>0} .$$

The IG subordinator is an infinite activity Lévy process because the total mass of the Lévy measure is infinite:

$$\int_0^\infty \ell_Z(z)dz = \infty .$$

The IG subordinator is a Lévy process of infinite variation because it satisfies:

$$\int_{|z|<1} |z| \, \ell_Z(z)dz = \infty ,$$

which can be further simplified as follows since subordinators have only positive jumps:

$$\int_{(0,1)} z\ell_Z(z)dz = \infty .$$

Consult theorem 3.11 of Matsuda (2005a).

A.3 Lévy-Khinchin Representation

The following theorem is from Matsuda (2005a). Also consult theorem 8.1 of Sato (1999).

Theorem: General Lévy-Khinchin representation (formula) of all Lévy processes (processes whose increments follow infinitely divisible distributions) Let $(X_{t\in[0,\infty)})$ be a real valued Lévy process defined on a filtered probability space $(\Omega, \mathcal{F}_{t\in[0,\infty)}, \mathbb{P})$. Then, the characteristic function $\phi_X(\omega)$ of a Lévy process $(X_{t\in[0,\infty)})$ can be expressed as:

$$\phi_X(\omega) = \exp\left(t\psi_X(\omega)\right),$$

where $\psi_X(\omega)$ called a characteristic exponent (or a log characteristic function) is given by:

(A.5) $$\psi_X(\omega) = -\frac{A\omega^2}{2} + i\gamma\omega + \int_{-\infty}^{\infty} \left\{ \exp(i\omega x) - 1 - i\omega x 1_{|x|\le 1} \right\} \ell(dx),$$

where A is a unique nonnegative constant (i.e. $A \in \mathbb{R}^+$), γ is a unique constant on $\mathbb{R}$, and ℓ is a unique measure on $\mathbb{R}$ satisfying:

$$\ell(\{0\}) = 0 \text{ and } \int_{-\infty}^{\infty} \min\{|x|^2, 1\}\ell(dx) < \infty .$$

Proof

Consult Sato (1999) p.37-p.47.

Because the tails of the Lévy measure of the CGMY process (34) are exponentially decayed, we can use a special case of the general Lévy-Khinchin representation without the truncation of large jumps.

Theorem: Lévy-Khinchin representation of Lévy processes without truncation of large jumps Let $(X_{t\in[0,\infty)})$ be a real valued Lévy process defined on a filtered probability space $(\Omega, \mathcal{F}_{t\in[0,\infty)}, \mathbb{P})$. Then, the characteristic function $\phi_X(\omega)$ of a Lévy process $(X_{t\in[0,\infty)})$ without the truncation of large jumps can be expressed as:

$$\phi_X(\omega) = \exp\left(t\psi_X(\omega)\right),$$

where the characteristic exponent $\psi_X(\omega)$ is given by:

(A.6) $$\psi_X(\omega) = -\frac{A\omega^2}{2} + i\gamma\omega + \int_{-\infty}^{\infty}\left\{\exp(i\omega x) - 1 - i\omega x\right\}\ell(dx),$$

where A is a unique nonnegative constant (i.e. $A \in \mathbb{R}^+$), γ is a unique constant on $\mathbb{R}$, and ℓ is a unique measure on $\mathbb{R}$ satisfying:

$$\ell(\{0\}) = 0 \text{ and } \int_{-\infty}^{\infty}\min\{|x|^2, 1\}\ell(dx) < \infty.$$

References

Bakshi, G., Cao, C., and Z. Chen. “Empirical Performance of Alternative Option Pricing Models.” *Journal of Finance*, 52 (1997), 2003-49.

Barndorff-Nielsen, O. E. “Exponentially Decreasing Distributions for the Logarithm of the Particle Size.” *Proceedings of the Royal Society of London*, A353 (1977), 401-419.

Barndorff-Nielsen, O. E., and O. Halgreen. “Infinite Divisibility of the Hyperbolic and Generalized Inverse Gaussian Distributions.” *Zeitschrift für Wahrscheinlichkeitstheorie und verwandte Gebiete*, 38 (1977), 309-312.

Barndorff-Nielsen, O. E. “Processes of Normal Inverse Gaussian Type.” *Finance and Stochastics*, 2 (1998), 41-68.

Barndorff-Nielsen, O. E. ed. Lévy Processes: Theory and Applications. Birkhäuser (2001).

Bates, D. “Jumps and Stochastic Volatility: Exchange Rate Processes Implicit in Deutschemark Options.” *Review of Financial Studies*, 9 (1996), 69-108.

Black, F., and M. Scholes. “The Pricing of Options and Corporate Liabilities.” *Journal of Political Economy*, 81 (1973), 637-654.

Breeden, D. T., and R. H. Litzenberger. “Prices of State-Contingent Claims Implicit in Option Prices.” *Journal of Business*, vol. 51, issue 4 (1978), 621-651.

Carr, P., Chang, E. C., and D. B. Madan. “The Variance Gamma Process and Option Pricing.” *European Finance Review*, 2 (1998), 79-105.

Carr, P., Geman, H., Madan, D. B., and M. Yor. “The Fine Structure of Asset Returns: An Empirical Investigation.” *Journal of Business*, vol 75, issue 2 (2002), 305-332.

Carr, P., and D.B. Madan. “Option Valuation Using the Fast Fourier Transform.” *Journal of Computational Finance*, 2 (1998), 61-73.

Cont, R. “Empirical Properties of Asset Returns: Stylized Facts and Statistical Issues.” *Quantitative Finance*, 1 (2001), 1-14.

Cont, R., and P. Tankov. Financial Modelling with Jump Processes. Chapman & Hall/CRC Financial Mathematics Series, (2004).

Derman, E., and I. Kani. “Riding on a Smile.” *Risk 7*, (1) (1994), 18-20.

Dumas, B., Fleming, J., and R.E. Whaley. “Implied Volatility Functions: Empirical Tests.” *Journal of Finance*, 53, No.6 (1998), 2059-2106.

Dupire, B. “Pricing and Hedging with Smiles.” Working Paper (1993), Swaps and Options Research Team, Paribas Capital Markets.

Dupire, B. “Pricing with a smile,” *Risk*, 7 (1994), 18-20.

Eberlein, E., and U. Keller. “Hyperbolic Distributions in Finance.” *Bernoulli*, 1 (1995), 281-299.

Eberlein, E., Keller, U., and K. Prause. “New Insights into Smile, Mispricing, and Value at Risk: The Hyperbolic Model.” *Journal of Business*, Vol. 71 Issue 3 (1998), 371-405.

Harrison, J. M., and S. R. Pliska. “Martingales and Stochastic Integrals In the Theory of Continuous Trading.” *Stochastic Processes and Applications*, 11 (1981), 215-260.

Harrison, J. M., and S. R. Pliska. “A Stochastic Calculous Model of Continuous Trading: Complete Markets.” *Stochastic Processes and Applications*, 15 (1983), 313-316.

Heston, S. L. “A Closed-Form Solution for Options with Stochastic Volatility with Applications to Bond and Currency Options.” *Review of Financial Studies*, 6 (1993), 327-343.

Honoré, P. “Pitfalls in Estimating Jump-Diffusion Models,” Working Paper Series No. 18 (1998), CAF Aarhus School of Business, University of Aarhus.

Hull, J. C., and A. White. “The Pricing of Options on Assets with Stochastic Volatilities.” *Journal of Finance*, 42 (1987), 281-300.

Koponen, I. “Analytic Approach to the Problem of Convergence of Truncated Lévy Flights Towards the Gaussian Stochastic Process.” *Physical Review E*, 52 (1995), 1197-1199.

Matsuda, K. “Dynamics of Risk-Neutral Densities Implied By Option Prices.” Working Paper (2004a), Graduate School and University Center of the City University of New York.

Matsuda, K. “Introduction to Option Pricing with Fourier Transform: Option Pricing with Exponential Lévy Models.” Working Paper (2004b), Graduate School and University Center of the City University of New York.

Matsuda, K. “Introduction to the Mathematics of Lévy Processes.” Working Paper (2005a), Graduate School and University Center of the City University of New York.

Merton, R. C. “Theory of Rational Option Pricing.” *Bell Journal of Economics and Management Science*, 4 (1973), 141-183.

Merton, R. C. “Option Pricing When Underlying Stock Returns Are Continuous.” *Journal of Financial Economics*, 3 (1976), 125-144.

Prause, K. “The Geenralized Hyperbolic Model: Estimation, Financial Derivatives, and Risk Measures.” PhD Thesis (1999), Universität Freiburg.

Raible, S. “Lévy Processes in Finance: Theory, Numerics and Empirical Facts.” PhD Thesis (1998), Universität Freiburg.

Sato, K. Lévy process and Infinitely Divisible Distributions. 1999, Cambridge University Press.

Wilmott, P. Derivatives. 1998, John Wiley & Sons.